UNIVERSITÀ DI SIENA 1240

Department of Medical Biotechnology

Doctorate in Genetics, Oncology and Clinical Medicine
GenOMeC

XXXVI Cycle (2020-2023)

Coordinator: Prof. Ilaria Meloni

Proapoptotic effects of miR-204 inhibition in melanoma cell lines and in melanoma models *in vivo*

Disciplinary scientific sector: *BIO/11 - Molecular Biology*

Supervisor

Dr. Laura Poliseno
(CNR di Pisa)

PhD candidate

Antonella Prantera
(CNR di Pisa)

Academic year
2022/2023

Summary

Abstract

Proapoptotic effects of miR-204 inhibition in melanoma cell lines and in melanoma models *in vivo*

MicroRNAs are small molecules of non-coding RNA and they play a relevant regulatory activity in carcinogenesis, during both development and progression steps. In my thesis, I focused on miR-204 which, in melanoma cells, is negatively regulated by $BRAF^{V600E}$ through the ERK pathway.

Although it belongs to the same family as miR-211, miR-204 exerts a different biological role. When it is overexpressed, it shows an oncosuppressive function, in particular, it causes a decrease in cell migration/invasion by repressing AP1S2 gene.

During the 3 years of my PhD project, I studied the effects associated with miR-204 inhibition. Following miR-204 inhibition through the transfection of LNA-204, I unexpectedly observed a significant decrease in cell proliferation, a decrease in cell ability to form colonies and a strong increase in apoptosis *in vitro*. In addition, I confirmed the antiproliferative and proapoptotic effects in *in vivo* model systems (zebrafish embryos, nude mice and genetically engineered melanoma mouse model). The biological results are specifically due to miR-204 inhibition (not to miR-211 inhibition).

Then, I demonstrated that the apoptosis due to miRNA inhibition is dose dependent, using the A375 sgRNA miR-204 melanoma line, in which the amount of endogenous miRNA is reduced by the CRISPR-Cas9 technique compared to the control line (A375 sgRNA AVV1).

In addition, I performed the caspase assay and quantified the activity of caspase 3/7, caspase-8 and caspase-9 in order to understand which pathway mediates the apoptotic phenotype. The experimental data suggest that there is not a predominant pathway, but both (intrinsic and extrinsic) are activated at 18h after LNA transfection.

I also investigated the molecular mechanism through which the apoptosis occurs. In this regard, at 6h from cell transfection, I measured an increment in p53 protein level in several melanoma cell lines and I concluded that cell death is correlated to p53 signaling.

Considering the early induction of p53, I aimed to identify one or more miR-204 specific targets and, for this purpose, I performed an RNA-Seq at 6h post transfection of LNA-204-MM or 204 in A375 and 501Mel cells. By analysing the sequencing data, I obtained a short

list of candidate genes. It includes ATP2A1, IQCN, RCVRN (involved in calcium signaling) and ACTA1, MYH3 (related to adhesion/migration processes). Indeed, at 6h post transfection of LNA-204, I observed an increment in calcium concentration and a decrease in cell adhesion. To date, I'm proceeding with the characterization of each candidate gene in order to understand whether they are direct targets of miR-204 and what is their role in the phenomenon studied. In line with the results already obtained I am exploring different aspects: the interaction p53-ATP2A1 at the ER level, the loss of adhesion and the possible involvement of TRPM3 (miR-204 host gene). Furthermore, I will try to understand whether and how calcium signaling affects these different mechanisms.

In conclusion, by promoting apoptosis in a dose-dependent manner, LNA-204 could be exploited as a drug in order to develop a new therapeutic strategy for the treatment of melanoma.

1. Introduction

Epidemiological aspect, risk factors and therapeutic strategies for the treatment of cutaneous melanoma

1.1. Cutaneous melanoma

Cutaneous melanoma is an aggressive form of skin cancer. It arises from the neoplastic transformation of melanocytes, cells originated from neural crest and located in the basal layer of the epidermidis. Melanocytes play a significant role when UV- induced DNA alteration occurs, in particular they are responsible for the production and the release of melanin pigment that protects cells from UV and therefore prevents ulterior DNA damage [1]. This type of cancer is very common in the elderly, even if many cases are detected in patients of the age of 15 and 39 years and the localization is related to the gender, in particular it appears in the lower legs in woman and on the head and neck in men.

In the early 1900s few cases of cutaneous melanoma were diagnosed (1 in 500 individuals), but during the last decades the incidence rate significantly increased due to the major recognition of the disease and early diagnosis [2]. Nowadays, the highest incidence is in the Caucasian populations in which, effectively, melanoma and its clinical, pathogenetic and histological features have been studied [3]. On the European continent the incidence rate is high in the countries of North and low in the countries of South (in Italy every year 5-7 cases of melanoma per 100,000 inhabitants). A possible explanation is that the Southern European populations have a more pigmented skin, so they are more protected against UV then the Southern people [4]. Conversely, the incidence is low in African people and the rarity is attributed to the relevant content of melanin that which exerts a protective effect from UV radiations [3].

1.1.1. The most important risk factors in melanoma etiopathogenesis

Cutaneous melanoma is defined multifactorial disease inasmuch its development depends on environmental and host (genetic) risk factors. Regarding environmental factors, the most

important is the exposure to ultraviolet rays (UVA, UVB, UVC). However, the increased risk of developing melanoma is mainly due to the genotoxic effect of UVA and UVB radiations [4]. UVA causes DNA damage in indirect manner, in particular, their penetration into the skin follows the transfer of energy to the oxygen molecules with the formation of reactive chemical species [2]. This kind of radiation can also derive from artificial sources such as tanning bed, categorized as human carcinogen, or photochemotherapy treatment to which patients affected by psoriasis are subjected [4]. Many studies revealed a correlation between the use of sunbed and the development of melanoma especially in young individuals [1]. Instead, the exposure to UVB induces the formation of pyrimidine dimers which directly damage DNA causing apoptosis, but it has been seen that an intermittent and intense exposure is associated with melanoma, while a chronic exposure is associated with non-melanoma skin cancers [2]. Also host risk factors play a role in melanoma etiopathogenesis. One of the most important is the number of melanocytic nevi, classified as benign lesions composed of melanocytes accumulation. The risk for melanoma is higher in individuals with more than 100 nevi. Nonetheless, analysing the histology of melanoma samples, in most cases the cancer is thought to originate *de novo* and only 20-30% seems to derive from a precursor nevus (NAM). Probably, it's complicated to detect the nevus component because the tumor component destroys or obscures it and consequently NAMs are underestimated. Other host risk factors are the family history (5-10% of melanomas) [2] and the genetic predisposition (melanoma appears at a younger age). Furthermore, a higher risk of developing melanoma has been found in individuals with particular phenotypic traits such as freckles, light skin, red hair, sun susceptibility, light eyes.

1.1.2. The development of malignant melanoma: biological, molecular and genetic aspects

Cutaneous melanoma arises following a process of neoplastic transformation that affects melanocytes. The melanocytes, derived from neural crest cells, are distributed in various body sites, including the basal layer of epidermidis, and they ensure photoprotection as they are characterized by the presence of granules, the *melanosomes*, containing melanin (pheomelanin and eumelanin). In physiological conditions the keratinocytes produce MSH (melanocyte stimulating hormone) which binds to the receptor MC1R (melanocortin receptor 1) expressed on the membrane of melanocytes, stimulating their proliferation and the release of melanin. The level of melanin synthesized in melanosomes defines skin colour and easiness of tanning,

the so-called "skin phenotype" [5], but the most important role of this pigment is to shield UV radiation, preventing DNA damage [1]. Therefore, the amount of melanin can be considered a factor predicting melanoma risk since UVA irradiation represents the main factor that triggers melanocytes malignant transformation [5]. The development of melanoma can occur through two mechanisms. The first mechanism consists in the direct transformation of melanocytes in cancer cells following various mutations affecting oncogenes and tumor suppressor. The alternative mechanism consists in the transformation of melanocytes in benign nevi. In most cases, they carry $BRAF^{V660E}$ mutation, but this single mutation is not enough for the onset of melanoma whereby the nevi remain indolent for years thanks to the surveillance of immune system, but the intermittent UV irradiation can cause the acquisition of further DNA alterations leading to carcinogenesis.

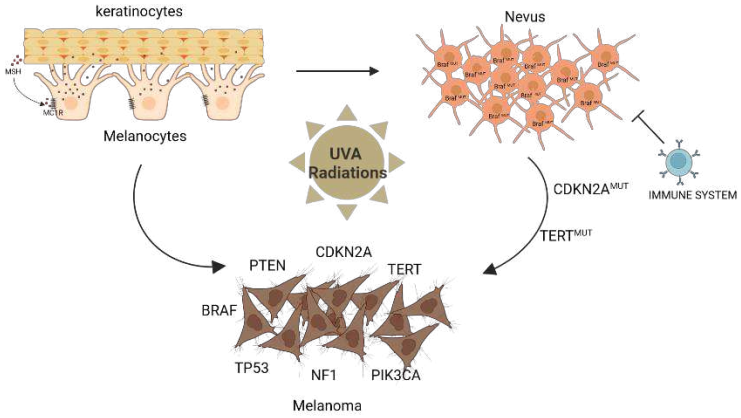

Figure 1. The mechanisms through which the development of melanoma occurs.
The picture summarizes the two mechanisms that promote the transformation of melanocytes in cancer cells following exposure to UVA radiations: the direct process due to mutations affecting oncogenes and tumor suppressor and an indirect transformation through the formation of benign BrafV600E nevi which can remain indolent or accumulate further mutations initiating the carcinogenesis.
It is readapted from *Leonardi et al. (2018)* and created with *Biorender.*

The mutational profile of melanoma is heterogeneous: the genetic mutations affect genes involved in numerous cellular processes and, in 90% of cases, their presence causes the aberrant activation of MAPK pathway which plays a central role in the transduction of cell proliferation, differentiation and survival signals [1]. In cancer cells the signaling pathway is not regulated, as in healthy cells, and it results constitutively active. The downstream effects of dysregulation are several (increased proliferation, increased viability, inhibition of FAS-dependent cell death) and they imply the development and the progression of tumor mass [6]. As in other cancers, in melanoma cells the abnormal activation of MAPK pathway is, mainly, due to BRAF missense mutations. More than 90% occur in codon 600 of the serine-threonine protein kinase and the most common is *V600E* mutation which determines the substitution of

valine with glutamic acid [7]. Due to the replacement of a hydrophobic amino acid with a polar one, $BRAF^{V600E}$ assumes a constitutively active conformation and, consequently, it has an enzymatic activity higher than the wild-type protein causing the aberrant functioning of the pathway and the effects described previously. Abnormal MAPK signaling can be associated with NRAS mutations following which the protein remains in its active form (GTP- bound) for longer. However, has been seen that, in rare cases, BRAF and NRAS mutations coexist because they are mutually exclusive [1].

Although the genetic heterogeneity, for the treatment of melanoma, the main therapeutic target is represented by BRAF, in particular $BRAF^{V600E}$, as it is the most frequent mutation in patients. In clinic, the first $BRAF^{V600E}$ inhibitor was Vemurafenib. Following the administration of vemurafenib the response to the drug is effective, but in 50% of patients, within 6-8 months from the start of treatment, melanoma cells acquire resistance to BRAFi and there is a resumption of tumor growth [8]. The mechanisms associated with resistance are several, including the appearance of mutations *de novo* in the other kinases of MAPK pathway, errors leading to the formation of new $BRAF^{V600E}$ splicing variants [9] and PTEN loss of function which results in PI3K/AKT pathway aberrant activation [1].

Nowadays, for the treatment of melanoma various options are available (surgical excision, radiotherapy, chemotherapy, immunotherapy and targeted therapy) [10]. Regarding targeted therapy, the adjuvant therapy is preferred to the use of a single therapeutic agent as has been seen that the combination of BRAFi and MEKi delays the acquisition of cell resistance [9]. Furthermore, following the Covid-19 pandemic, which made it possible to observe the positive effects of mRNA vaccines in the world population, the interest of the scientific community in the use of mRNA vaccines for the treatment of various types of cancer, including melanoma, has grown. mRNA vaccines contain a mRNA encoding for neoantigens (exclusively expressed by tumor cells), tumor-associated-antigens or mediators of the inflammatory process. Therefore, their function is to enhance the immune response against the tumor [11]. To date, clinical trials are underway to test various mRNA vaccines against melanoma. However, further studies are necessary to increase its effectiveness in humans, in particular to ensure that the $CD8^+$ T cells response is strong as that stimulated in animal models [12].

In addition to genetic mutations, many studies have revealed that melanoma microenvironment is altered, in particular it is characterized by the overexpression of metalloproteinases (MMP-9 and MMP-2). These proteins degrade the extracellular matrix, promoting the metastasis process; accordingly their action determines the high metastatic power of cutaneous melanoma [1].

1.2. MicroRNA and melanoma

In recent decades many studies have shown that the process of carcinogenesis is associated with an altered expression of genes and non-coding sequences including microRNA. Mature microRNA (miRNA) are small non-coding RNA molecules (22 nucleotides) and, in general, are encoded by sequences located in the introns of host genes. They act as regulators of gene expression, in particular, pairs completely or incompletely with a mRNA sequence and, based on degree of complementarity, they inhibit the translation of the transcript or induce its degradation. Normally, the interaction miRNA-mRNA is established between the *seed region* (a sequence consisting of 7 nucleotides and located at the 3') of the miRNA and the 3' UTR of mRNA target, but in some cases the miRNA can bind to the 5' UTR or coding sequence [13]. Recently, it has been demonstrated that microRNAs are, also, able to regulate the expression of other miRNAs, in direct or indirect manner. The direct interaction occurs in the cytoplasm between two mature miRNAs or in the nucleus between a pri-miRNA and a mature one. Therefore, a miRNA can auto-regulate and decreases its level, controlling its immature form. Instead, the indirect regulation occurs through the suppression of transcription factors or components involved in biogenesis process of the miRNA target [14].

In melanoma, as in other cancers, miRNAs regulate numerous processes such as apoptosis, migration, proliferation [15]. Another interesting aspect is their relevant role in the acquisition of resistance to BRAFi through the reactivation of MAPK pathway [16], and the involvement in immune escape implemented by melanoma cells. In particular, it has been seen that cancer cells release exosomes containing microRNAs which play a role in different mechanisms. For example, they reduce the immune response altering $CD8^+$ T-cells function[17], inducing the transformation of fibroblasts in CAFs (Cancer-associated fibroblasts), modulating the production and the release of cytokines or making tumor cells resistant to the action of Natural killers cells [18]. Since the expression of some miRNAs is significantly different when comparing the serum and plasma of people affected by melanoma with those of healthy people, circulating miRNAs derived from the exosomes could be used as diagnostic and prognostic markers (in order to distinguish patients with stage I-II melanoma and those at stage III-IV). However, the definition of a miRNAs panel to use for melanoma diagnosis and prognosis is difficult because various factors can interfere. It remains a challenge for the future![15]. In addition, the concentration of some miRNAs in the extracellular environment can be exploited to predict the efficacy of therapeutic treatment, in particular the response to BRAFi [10].

As previously mentioned, MAPK pathway is one of the most important in melanomagenesis. A lot of microRNAs are regulated by BRAF signaling and they have been identified by

comparing melanocytes and $BRAF^{V600E}$ melanoma cell lines before and after the treatment with MEKi or BRAFi. One of them is miR-204 [16] [19] [20] that represents the focus of my PhD project.

1.2.1. MiR-204-5p: a regulator in physio-pathological processes and cancer

MiR-204-5p (to simplify miR-204) is classified as an intronic miRNA because its encoding sequence is contained in intron 6 of *TRPM3* (Transient Receptor Potential Mestatin 3). *TRPM3* gene codifies for a cationic channel, located on plasmatic membrane, that allows Ca^{2+} and Zn^{2+} to enter inside the cell; it acts as tumor-promoter, which is why it is overexpressed in many tumors, and is a miR-204 validated target.

In presence of stimuli that induce the expression of miR-204 and host gene, and probably also in physiological conditions, the cells implement a regulatory mechanism through which miR-204 downregulates *TRPM3* to prevent its oncogenic activity[21]. This regulation leads to a negative correlation between miR-204 (tumor suppressive function) expression e and TRPM3 protein (oncogene) level: in healthy tissue there is, generally, a higher expression of miRNA and lower levels of the protein compared to cancer where miR-204 expression is downregulated and TRMP3 protein levels are elevated. The molecular mechanism has been studied in clear cell renal cell carcinoma (ccRCC) in which TRPM3 stimulates autophagy, decreasing the effectiveness of anti-angiogenic therapies and supporting tumor growth. The authors of paper demonstrated that miR-204 suppresses the expression of TRPM3 directly or indirectly (targeting CAV1): when miRNA is inhibited, using an anti-miR-204, the accumulation of TRPM3 protein is observed, on the contrary, overexpressing the miRNA, the level of the protein decreases [22]. Furthermore, a study has revealed that in hepatocellular carcinoma miR-204 is able to bind lcnRNA HOTTIP, repressing its expression. This is an example of a short non-coding RNA that regulates the expression of a long non-coding RNA [21].

The microRNA of my interest has an essential function in several physio-pathological conditions: it is overexpressed in retinal pigment epithelium where tags factors involve in eye development and regulates the adipogenesis [23]. In addition, it plays a key role in diabetes as inhibits the production of insulin in pancreatic β-cells. Regarding the cancerous context, different types of human cancers have been analysed and most studies have shown that miR-204 acts as onco-suppressor, a its expression is, importantly, downregulated. The miRNA hinders carcinogenesis and tumor progression through several mechanisms. Commonly, miR-204 promotes the apoptosis by inhibiting the expression of anti-apoptotic proteins [21] as seen

in hepatocellular carcinoma (BCL-2, NUAK1, SIRT1, SIX1) and intrahepatic cholangiocarcinoma (BCL-2, SLUG) [23]. Another onco-suppressive strategy is the repression of EMT (epithelial-mesenchymal transition), a biological process during which epithelial cells, immotile and polarized, acquire new molecular and phenotypic characteristics, and evolve to motile mesenchymal cells, capable of migrate and form metastases. In this case, miR-204 targets inhibition leads to a reduction in adhesion proteins level, an increase in specific proteins of mesenchymal cells and the activation of factors associated with metastasis formation [21]. This mechanism occurs in a variety of cancers. For example, in breast cancer miR-204 supresses EMT and bone metastasis by tagging IL-11, SOX4 and SIX1 [21], in gastric cancer cells the miRNA impedes the metastatic process and EMT by inhibiting SIRT1 expression [23], while in oesophageal cancer miR-204 target is FOXM1, an activator of EMT [21]. In addition to the tumors already mentioned, the onco-suppressive role of miR-204 has also been demonstrated in glioma, osteosarcoma, renal cell carcinoma, cervical cancer, pancreatic cancer, lung cancer, colorectal cancer in which it negatively regulates several biological processes such as survival, proliferation, migration, invasion and angiogenesis, by inhibiting the expression of genes related to the PI3K/AKT. A further interesting thing, emerged from numerous research and related to its anti-tumor activity, is that miR-204 sensitizes cancer cells to chemotherapeutic agents [23]. Particularly, in gastric cancer, it has been seen that, by overexpressing miR-204, the cells are more sensitive to treatment with 5-fluorouracil.

Although mir-204, mainly, has a tumor-suppressive activity, in literature studies have been published in which has been demonstrated how this miRNA can act both as a tumor-suppressor and as a oncomiR. This dual role has been characterized in prostate cancer where miRNA is downregulated by androgen and its role varies between cell lines depending on the expression of the hormone receptor. In prostatic adenocarcinoma (PAC) cells (LNCaP and 22RV1) which express the receptor, the expression of miR-204 is lower than in neuroendocrine-like prostate cancer (NEPC) cells (PC-3 and CL1) without AR. In the first cell lines mir-204 inhibits cell growth and clonogenicity both *in vitro* and *in vivo*, therefore it acts as a tumor-suppressor; on the contrary, in the second one the microRNA has an oncogenic activity as it promotes cell growth and clonogenicity[21]. Breast cancer and ovarian cancer are other tumors in which miR-204 is overexpressed and plays a tumor-promoter role [23] .

1.2.2. The already known role of miR-204 in melanoma cells

In a precedent paper on melanoma, published by Poliseno's research group, miR-204 has been identified among miRNAs upregulated by vemurafenib (BRAFi), a selective inhibitor of $BRAF^{V600E}$, and by trametinib (MEKi). In fact, the authors demonstrated that mutated BRAF represses miR-204 expression through ERK pathway.

MiR-204 belongs to the same family as miR-211. Both are intronic microRNAs and are, respectively, located in intron 6 of TRPM3 and TRPM1. Although miR-211 expression is promoted by BRAi and MEKi like miR-204, their induction was found to be mutually exclusive. In amelanotic cell lines, which express only miR-204, following treatment with drugs, it is logically induced; in melanotic lines they are co-expressed, but the treatment with vemurafenib and trametinib leads to an increase in TRPM1/miR-211 level. These data indicate that, downstream of MAPK pathway, the two miRNAs are subject to a different transcriptional regulation. Effectively, miR-211 transcription is activated by MITF, while miR-204 upregulation is STAT3 dependent. One more difference between the miRNAs in question is linked to the expression. MiR-204 is ubiquitously expressed, instead the expression of miR-211 represents a peculiar feature of melanocytic lineage. Thus, melanoma in the unique cancerous setting in which both are present and play a biological role.

Even if miR-204 and miR-211 are members of the same family and, sharing the seed region, have many target genes in common, they not only show distinct characteristics from each other, but also perform a dissimilar activity. The authors of paper demonstrated that, once induced, miR-211 causes an increment in TYR protein levels, a crucial enzyme in melanin biosynthesis process, promoting cell pigmentation and the upregulation of TYR is due to the repression of EDEM1 that mediates the protein translocation into the cytoplasm and its degradation. As is known, pigmentation represents an adaptive mechanism that confers resistance to melanoma cells because melanosomes can retain drugs and liberate them into the external environment. In conclusion, miR-211 overexpression has a negative effect on cell proliferation, but at the same time, with its pro-pigmentation activity, it limits the antiproliferative action of vemurafenib and increases cell sensitivity to the drug. Nevertheless, in this condition the efficacy of vemurafenib improves when administered in combination with a pigmentation inhibitor such as PTU. On the contrary, when the miRNA is inhibited, an increase in cell proliferation is observed, but the effectiveness of BRAFi increases. The role of miRNA just described is supported by patient data. It has been seen that patients with metastatic and melanotic tumors are less responsive to BRAFi and MEKi therapy and, in addition, the higher TRPM1/EDEM1 ratio is associated with the lower survival rate.

Regarding miR-204, it is induced in amelanotic cell lines where melanin biosynthesis doesn't occur and therefore it cannot promote the pigmentation like miR-211. In fact, miR-204 exerts the tumor-suppressive role causing a reduction in the migration and invasive capacity of melanoma cells. The data obtained allow us to assert that miR-204 mediates the anti-motility activity of vemurafenib and the AP1S2 gene has been identified as the target through which it carries out this function [20]. Beyond to AP1S2, another target associated with the adverse effect on invasion is MMP9 [24].Contrarily, when miRNA expression is downregulated, using Crisp-CAs9, an increase in cell migratory ability is observed. However, it has been seen that miR-204 does not cooperate with vemurafenib because it has no effect on cell proliferation or ability to form colonies.

The tumor-inhibitor activity of mir-204, manifested through the impairment of migration/invasion is clinically confirmed. In more detail, Kaplan-Meier survival analysis shows that in patients with metastatic cancer and a higher TRPM3/AP1S2 ratio the survival rate is higher than in patients in whom the ratio is lower. MiRNA overexpression is associated with a better prognosis as it hinders tumor progression, regulating the expression of a large number of genes involved in as many biological processes [20]. This protective role provides an explanation for the fact that it is downregulated in melanoma compared to benign nevi and in metastatic tumors compared to primary ones [24].

In summary, despite miR-204 and miR-211 belong to the same family and, as expected, a copious number of genes have binding sites in their 3' UTR for both one and the other microRNA. For example, AP1S2 can also be targeted by miR-211 as well as EDEM1 by miR-204. Nonetheless, in melanoma they play a different role. This indicates that the activity of each miRNA depends, not only on the type of target and the capacity to regulate its expression, but also on the cellular context in which the miRNA is induced [20].

1.3. MicroRNAs as therapeutic targets

As has been widely discussed, microRNAs play a crucial role in the process of carcinogenesis, particularly during the initiation and progression phases [25]. They represent potential therapeutic targets since, by manipulating their expression within cancer cells, that of interacting genes can be indirectly modulated [13]. The modulation of miRNAs is advantageous because these are stable molecules, with a low molecular weight [23] and capable of acting on genes and, therefore, on proteins that cannot be affected by commonly administered drugs [13]. For this purpose, currently in preclinical studies, exogenous miRNAs are used. They can be divided into two groups: *miRNA mimics* and *miRNA inhibitors*. The first

are used to overexpress an endogenous miRNA that is downregulated in tumor and restore its biological activity. In order for these molecules to play their function, they must be synthesized as a double-stranded oligonucleotide with structural modifications that make them more stable and capable of recognizing the target mRNAs. On the other hand, miRNA inhibitors serve to downregulate endogenous miRNAs that are upregulated in cancer cells as they are associated with cancer development and progression. The most common strategy to inhibit an endogenous miRNA is to use an ASOs also know antagomir: they are single-stranded molecules complementary to the sense strand of the target miRNA. Very often, structural modifications are inserted to increase affinity, as in the case of LNAs (Locked Nuclei Acid). Other inhibitors are the so-called PNAs which are very resistant to the action of degradation enzymes as they match the entire miRNA sequence according to specific Watson-Crick recognition, and miRNA sponges which are conveyed into the cell through transgenic vectors under the transcriptional control of strong promoters. They exhibit the inhibitory action by binding to the seed region (7 nucleotides) of the miRNA in a complementary manner and, thus, specifically inhibit a single miRNA or those that, belonging to the same family, share the heptameric sequence [13].

1.3.1. Locked Nucleic Acid oligonucleotides

Among miRNA inhibitors, LNAs (Locked Nucleic Acid) are the most used, both *in vitro* studies and *in vivo* models. These are RNA analogous in which the 2'-oxygen of ribose is connected to 4'-carbon by a methylene group assuming a "locked" conformation that confers rigidity, while the bases are linked to a skeleton of phosphate as occurs in conventional nucleic acids. In fact, LNAs can pair to complementary DNA or RNA sequences (according to the Wahtson-Crick rules), forming heteroduplexes [26]. They possess important properties, reason why their use confers numerous advantages compared to traditional oligonucleotides. It has been seen that they have a greater affinity for the target, are more sensitive and specific and, following hybridization with the complementary strand, they form more thermally stable LNA:DNA or LNA:RNA structures. Specificity, sensitivity and thermal stability can be optimized by modifying the number of LNA monomers in the oligonucleotide. For example, the T_m of the duplex can increase between 2-8 °C for each LNA monomer incorporated into the strand. As a result of this, it's possible to use LNA oligonucleotides that are shorter than DNA or RNA those, but still have an elevated T_m. All these properties make LNAs capable of discriminating between sequences that have a high similarity (up to one nucleotide difference) like in the case of mRNA or miRNA belonging to the same family, of recognizing very small

target sequences or whose levels are very low. Another relevant aspect that allows both *in vivo* and *in vitro* application is the greater resistance to the action of nucleases (exonucleases and endonucleases) compared to DNA and RNA oligos *(Quiagen page)*. However, this feature depends on the position of LNAs: a single modification at 3'-end of the oligonucleotide does not confer resistance, while two LNAs at the 3' or confer resistance to different types of exonucleases [27]. Instead, as regards physical properties like DNA and RNA, LNAs are soluble in water and this allows to adapt standard protocols to their use *(Quiagen page)*. Additionally, they can be easily transported into cells by means of positively charged lipid structures that bind to the negatively charged phosphate scaffold [26]. The lipids fuse with the cell membrane and release the oligos which from the cytoplasm are rapidly transported into the nucleus where RNase H is present. Nevertheless, the modified monomer is not able to activate the enzyme. For this to happen it is necessary to incorporate a DNA sequence into the oligo. In fact, LNA-DNA co-polymers recognize and bind the target sequence. At this point the DNA strand recruits RNase H which makes a cut in the DNA-RNA duplex degrading the mRNA. LNA inability to activate the enzyme is especially advantageous for *in vivo* use because it avoids the degradation of non-specific mRNAs to which the oligo pairs in a non-perfectly complementary manner. The properties of LNA discussed so far have been studied *in vitro* and then confirmed through *in vivo* studies. The data obtained in mice, comparing DNA and LNA oligos, indicate that the latter are more stable, have a higher affinity for the target and a lower toxicity than the others. Further, thanks to their function as antisense oligonucleotides, they are more effective in inhibiting tumor growth in cell cultures as well as in animal models [28].

1.3.1.1. LNA-204: a specific inhibitor of miR-204-5p

Based on the results emerged in the paper *Vitiello et al*. by overexpressing miR-204, to better characterize the role of this microRNA in melanoma cells a specific inhibitor (miRCURY LNA miRNA Inhibitor) was used which will simply be indicated with the acronym LNA-204. It is an antisense oligonucleotide that has a perfect sequence complementary to the miRNA of interest. Once transfected into cells, they bind to miR-204 forming highly stable heteroduplexes and prevents the interaction between miRNA and its intracellular targets.
Considering that the overexpression confirmed the tumor-suppressive role of miR-204 in melanoma cells, already seen in other tumors, LNA-204 was expected to have oncogenic effects, in particular causing an increase in cellular migration/invasion and more generally

promote tumor progression.In reality, the results obtained by inhibiting miR-204 are surprising!

2. Aim

My PhD project is focused on the study of LNA-204 proapoptotic effects. This molecule is used in melanoma cells in order to inhibit the endogenous miR-204.

In the paper *Vitiello et al.* (2017) the research group of Dr. Laura Poliseno has identified the miRNAs that in melanoma are regulated by $BRAF^{V600E}$ through the ERK pathway. Among them, I focused my attention on miR-204. Although miR-204 belongs to the same family as miR-211, it plays a different role and, furthermore, in melanoma, its role is expression-level dependent. miR-204 overexpression, through the repression of AP1S2 gene, causes a decrease in cell migration/invasion. Therefore, if overexpressed, it acts as a tumor-suppressor. Then, with the purpose to better characterize the activity of miR-204 in melanoma context, I inhibited it by using a specific LNA, the LNA-204. Contrary to expectations, following the inhibition I observed an increase in apoptosis. Based on these results, I supposed that miR-204 is an essential regulator of melanoma cells survival and, hence, its inhibition could represent an efficient anticancer therapy. My PhD project, that will be discussed in subsequent chapters, aimed:

1. to study the proapoptotic activity of LNA-204 in both cultured cells and *in vivo* models;
2. to demonstrate that miR-204 inhibition induces apoptosis in a dose dependent manner;
3. to investigate the extrinsic and intrinsic apoptotic pathways in order to understand which of them is activated;
4. to explore the molecular mechanism through which the apoptosis occurs;
5. to identify miR-204 direct target which, derepressed when the miRNA is inhibited, mediates the apoptotic phenotype.

3. Material and methods

3.1. Cell culture

Cells were grown at 37°C in a humidified atmosphere with 5% CO2. A375, B16F10, 501 Mel, M14, MeWo, SkMel-5, SkMel-28 melanoma cell lines were cultured in DMEM supplemented with 10% foetal bovine serum, 1% glutamine (Sigma-Aldrich) and 1% penicillin/streptomycin (Euroclone). A375 mCherry cell line were cultured in DMEM supplemented with 10% foetal bovine serum, 1% glutamine (Sigma-Aldrich) and 1% penicillin/streptomycin (Euroclone) supplied with 2uM of puromycin. A375 C2, A375 P2 and 501 Mel P1 vem-resistant cell lines were cultured in DMEM supplemented with 10% foetal bovine serum, 1% glutamine (Sigma-Aldrich) and 1% penicillin/streptomycin (Euroclone) supplied with 2uM of vemurafenib [20]. C-32 and A2058 cell line were cultured in EMEM supplemented with 10% foetal bovine serum, 1% glutamine (Sigma-Aldrich) and 1% penicillin/streptomycin (Euroclone). UACC62, COLO800 and NCI-H358 cell lines were cultured in RPMI supplemented with 10% foetal bovine serum, 1% glutamine (Sigma-Aldrich) and 1% penicillin/streptomycin (Euroclone). A375 AAV1 sgRNA and miR-204 sgRNA cell lines were generated as reported in [20] and were cultured in DMEM supplemented with 10% foetal bovine serum, 1% glutamine (Sigma-Aldrich) and 1% penicillin/streptomycin (Euroclone). HCT116 Dicer -/- were cultured in DMEM supplemented with 10% foetal bovine serum, 1% glutamine (Sigma-Aldrich) and 1% penicillin/streptomycin (Euroclone). A375-IQCN and A375-RCVRN cell lines were generated as reported afterwards and were cultured in DMEM supplemented with 10% foetal bovine serum, 1% glutamine (Sigma-Aldrich) and 1% penicillin/streptomycin (Euroclone).

3.2. Drugs

Cycloheximide (CHX, C4859-1ML), Doxycyclin hyclate (D-9891), Puromycin dihydrochloride (P8833), Z-4-idrossitamoxifene (4-HT, H6278) were purchased from Sigma. All drugs were diluted according to the manufacturer's instructions.

3.3. Oligos

PCR and qRT-PCR oligos and microRNA mimicking (mimics) were purchased from Eurofins Genomics (see Table 1, 2 and 3). LNA inhibitors were purchased from Exiqon (LNA-CT

339127YI00199006-AFA; LNA-204-MM 339141YCI0199919-ADA; LNA-204 339142YCI0200070-AFA; LNA-211 339141YCI0200071-ADA) (see Table 4).

Table 1. Sequence of PCR primers (cloning)

Gene	Forward primer (5'→3')	Reverse primer (5'→3')
IQCN	CATGTCGACGCCACCATGACCCTTCAA	ATGACGCGTCTAGATGCCAGGCCAATG
RCVRN	CATGTCGACGCCACCATGGGGAACAGC	ATGACGCGTTCAGGCGTTCTTCATCTTTTC
GFP-SEC61B	CATGCTAGCGCCACCATGGTGAGCAA	ATGACGCGTCTACGAACGAGTGTACTTGC

Table 2. Sequence of qRT-PCR primers

Gene	Forward primer (5'→3')	Reverse primer (5'→3')
ATP2A1	CCGGACCAAGTTAAGCGGAA	TCACCTTCCTCAAACCAGGC
AP1S2	CCTTGAGTGGCGAGATCTGA	CCTGATCCTCAATAGCACAGC
CHRNA10	AAGCTGTTCCGTGACCTCTT	CCACAGATACAGGGTCAGCA
GUCAB1	AGTACGTGGCAGCTCTGAAT	AAGATCCTGTCCACGACCTC
IQCN	GCAGAGCCAGGACAGTATCT	CGTCCACAGGTATGACAGGT
hsa-miR-204-family	TTC CCT TTG TCA TCC T	
RCVRN	GCAAGACCAACCAGAAGCTG	GCGTGTTTTCATCGTCTGGA

Table 3. Sequence of MicroRNA mimics

mimic	Sequence (5'→3')
si-CT moses	(GUCUGCGAUCGCAUACAAU)TT
204-mimic	(UUCCCUUUGUCAUCCUAUGCCU)TT
mimic-211	(UUCCCUUUGUCAUCCUUCGCCU)TT

Table 4. Sequence of LNAs

LNA	Sequence (5'→3')
LNA-CT	TAACACGTCTATACGCCCA
LNA-204-MM	GGCATTGGAAGACAAGGAGA
LNA-204	GGCATAGGATGACAAAGGGA
LNA-211	GGCGAAGGATGACAAAGGGA

3.4. Plasmids

Luciferase reporter vectors.

miR-204 family sensor. The pMiR-204 family sensor was generated cloning the fragment obtained from the alignment of miR-204-S-SpeI-BamHI-HindIII (5'-CTAGTAGGCATAGGATGACAAAGGGAAGGATCCA-3') and miR-204-AS-SpeI-BamHI-HindIII (5'-AGCTTTTCCCTTTGTCATCCTATGCCTGGATCCA-3') using SpeI/HindIII restriction sites. It was then subcloned into pMiR-report plasmid using SpeI/HindIII enzymes.

pTK. This plasmid expresses the Renilla Luciferase and it is cotransfected with miR-204 family sensor as normalization control.

Expression vectors.

LvEF1a-GCaAMP6s-T2A-Puro-WPRE. Lentiviral plasmid kindly given by Dr. F. Cremisi, CNR, Pisa, Italy and used to lentivirus transduction.

pCW-acGFP-SEC61B. GFP fusion to Sec61B was amplified from pcDNA3.1-GFP-SEC61B plasmid (kind gift from Prof. Carlotta Giorgi, Università di Ferrara, Italy) with Phusion Flash High-Fidelity Master mix (Thermo Fisher Scientific), using the primers listed in Supplementary Table 1. The PCR product was cutted with NheI and MluI and was cloned in the pCW vector previously digested with the same enzymes.

pCW-CTRL. The empty pCW vector was used as negative control for some infections.

pCW-IQCN. The CDS of IQCN was amplified from pcDNA3.1-3XFLAG-IQCN (kind gift from Dr. Chen Institute of Reproductive and Stem Cell Engineering, School of Basic Medical Science, Central South University, ChangSha, China) with Phusion Flash High-Fidelity Master mix (Thermo Fisher Scientific), using the primers listed in Table 1. For subsequent ligations, PCR products and pCW vector were digested with SalI and MluI restriction enzymes.

pCW-RVRN. The CDS of RCVRN was amplified from A375 cDNA with Phusion Flash High-Fidelity Master mix (Thermo Fisher Scientific), using the primers listed in Table 1. Then, the insert and the pCW vector were cutted with the appropriate restriction enzymes (SalI and MluI).

All restriction enzymes used for cloning were purchased from New England Biolabs.

3.5. Lentiviral transduction

pCW vectors were cotransfected in HEK293 cells (10^6 in 50mm plate) with 2 plasmids encoding proteins necessary for virus packaging, using Lipofectamine 2000™ (Thermo Fisher Scientific). After 48h, media containing lentivirus particles were harvested and they were centrifugated at 2500 *xg* for 5 minutes in order to pull down melanoma cells debris. Once

collected the supernatant containing lentivirus particles, melanoma cells were transduced with lentiviruses plus polybrene (4 ug/ml). Pools of stably transduced cells were selected by adding puromycin (2ug/ml) to the culture medium. 2ug/ml doxycycline was used in the experiments to induce transgene expression.

3.6. Transfection of miRNA mimics, LNAs and plasmids

Cells were seeded in 6well plates in order to reach 80%-90% confluency the day after or 48h after (stably infected cells treated with 2ug/ml of doxycycline). The indicated concentration of miRNA mimic, LNA or plasmids was added to 250 µl of incomplete medium, while 10 µl of 1 mg/ml of Lipofectamine 2000 (Thermo Fisher Scientific) were added to additional 250 µl of incomplete medium. Then, the two solutions were mixed together and the complexes (miRNA mimic/LNA/plasmids- Lipofectamine were allowed to form for 15 min at room temperature. In the meantime, the medium from each well was aspirated and replaced with 1.5 ml of fresh incomplete medium. The mixture was then added to the wells, let stand for 6h. 6h post-transfection, the medium was changed to complete medium and the cells processed according to the desired protocol.

3.7. Dead and alive cells

Cells ($2x10^5$) were seeded in 6 well plate. The day after they were transfected with LNAs and, at the indicated time point, the medium was collected in a tube and the adherent cells were detached using the trypsin. After a wash, the cells were centrifugated at 1200 *rpm* for 5 minutes and were resuspended in 500µl medium. 20 µl cellular suspension and 20 µl trypan blue were mixed in an eppendorf 1,5 and then, by loading 10 µl into the Burker chamber, the number of alive and dead (blue) cells was counted. The number of cells were graphed as percentage.

3.8. Growth curve assay at different time points

$3x10^3$ cells were seeded on 12-well plates, three wells per sample for each time point. The cells were transfected with LNAs and then, each time point was fixed with 2% PFA and stained using a crystal violet solution (0.1% crystal violet,20% methanol, in water). After the excess crystal violet solution was removed and the plates were washed with tap water and dried, cells were de-stained using a 10% acetic acid solution. Absorbance was then read at 590 nm (Chromate). Each sample was normalized on the vehicle-treated sample or on the negative

control sample and the data were graphed as variation of cell percentage among the different samples.

3.9. Cell cycle

$3x10^5$ cells were seeded in 100mm dishes. At the indicated time point, from the transfection of LNAs, cells were harvested with trypsin, and 10^5 cells were centrifugated at 1200 *rpm* for 10 minutes. After a wash with PBS, they were centrifugated again and were resuspended in 500µl PBS. Next, cells were fixed with 95% cold ethanol. They equilibrated at room temperature for 5 minutes and then 3 volumes PBS were added. Finally, were centrifugated as describes previously and stained with 300 µl propidium iodide solution (200 µg/ml P.I.; 0.1% NaCitrate, 0,5 mg/ml RNAse A, 0.1% Nonidet NP40). Once incubated at 4°C overnight, for each sample, 10.000 events were analysed by flow cytometry (C6 Accuri, BD).

3.10. Clonogenicity assay

Cells were seeded ($2x10^2$) in 6 cm plates in triplicate. After 8 days from the transfection with LNAs, cells were fixed and stained with a 0.1% crystal violet, 4% formaldehyde solution. The number of colonies was normalized on the number of colonies obtained in the negative control. The average colony number ± SEM for each group was then used to create a bar graph.

3.11. Adhesion assay

For cell attachment measurements, 24h post transfected cells were seeded on 12 well plates ($2x10^4$ cells/well in triplicates). At the indicated time point, plates are fixed and stained with crystal violet solution (0.1% crystal violet, 20% methanol, in water). Cells were counted and the number of each sample was normalized on the T=0.

3.12. Annexin V/PI assay

Melanoma cells ($2x10^5$) were seeded in 6well plate and the day after they were transfected with the reported LNAs. At the indicated time point the cells were washed with phosphate-buffered saline (PBS) and detached with cell dissociator. After a second wash in PBS, they were centrifugated at 400 *xg* for 5minutes, were stained with 80µl of a solution mix (in the dark) and, after 10 minutes of incubation at room temperature, for each sample, 10.000 events

were analysed by flow cytometry (C6 Accuri, BD). The solution mix is composed by 80µl buffer, 1,6 µl Annexin and 1,6 µl propidium (for each sample) as reported the manufacturer's instructions. Annexin-V-FLUOS staining kit (Roche, ref. #11988549001) were used.

3.13. Caspase activity assay

Melanoma cells ($5x10^4$) were seeded in 24 well and were transfected with the indicated concentration LNAs. 6h post-transfection the cells were seeded in 96-well plates at a density of $1,5x10^3$ cells/well in triplicates using the medium w/o cells as a control. Caspase activity was evaluated at the indicated time points according to the manufacturer's instructions and presented as a fold increase relative to the control. Caspase-Glo® 8 Assay kit (Promega, G8200), Caspase-Glo® 9 Assay kit (Promega, G8210) and Caspase-Glo® 3/7 Assay kits (Promega, G8091) were used.

3.14. Luciferase assay

Melanoma cells ($5x10^4$) were seeded in 24 well and were transfected with the indicated concentration LNAs. Luciferase activity was evaluated after 24h using the Dual-Luciferase® Reporter Assay kit (Promega, E1910) according to the manufacturer's instructions and presented as a fold increase relative to the control.

3.15. Xenograft in zebrafish embryos

6h after LNA transfection, A375 mCherry cells were prepared by mixing 10^6 cells with 2µl of MATRIGEL (Cultrex Basement Membrane Extract, PathClear), according to ref [29]. *Tg(Kdrl:EGFP)* ref nostra zebrafish embryos at 48hpf were anesthetizes with 0.04mg tricaine (#A-5040, Sigma-Aldrich) and grafted with 500 cells in the yolk sac. The fluorescence imaging was carried out 2 days after using the Nikon Eclips E600 microscope. The zebrafish embryos were carefully set down on glass slides embedded with 1% low melting agarose. The acquisitions were conducted with CoolSnap-CF camera using NIS-Elements software version 2.0 and the processing was completed by analyzing the area of tumors with ImageJ software (http://rsb.info.nih.gov). The rcmdr package of R software was used for statistical analysis.

3.16. Mice xenograft

6h after LNA transfection, A375 cells (10^4) were resuspended in DMEM/Matrigel (Corning) (1/1) and injected subcutaneously into both flanks of adult (8 weeks) female athymic nude mice (Foxn1 nu/nu) (Harlan Laboratories, Udine, Italy) (n=6 mice per group). Tumor volumes were measured once every 3 days using a caliper and calculated as (width)2 × length/2. The experiment was terminated on day 45, and then the tumors were weighted. Animals were monitored daily, housed in specific pathogen-free conditions and the experiment was approved by the Italian Ministry of Health in accordance with the Italian guidelines and regulations.

3.17. Mice strain

B6.Cg-Braftm1Mmcm Ptentm1Hwu Tg(Tyr-cre/ERT2)13Bos/BosJ mice were purchased from the Jackson Laboratory(013590). Tyr::CreER+ (heterozygousfor CreER), BrafCA/+ (heterozygous forBrafV600E), and Ptenlox/lox (homozygous for Pten loss) mice were used, as described in[30]. Mice were treated in compliance with the animal protocol #1180/2015-PR, initially approved by the Italian Ministry of Heath on November 16th 2015.

3.18. Histology and immunohistochemistry

Tissues were collected and fixed in 4% formaline for at least 48h. Then they were fixed and included in paraffin as reported in [30]. Sections of 5µm thickness were stained with Hematoxylin (05-M06002, Bio-Optica Milano Spa, Milan, Italy) and Eosin (05-B10003, Bio-Optica Milano Spa, Milan, Italy). Single immunostainings were performed on adjacent serial sections by using immunoperoxidase technique, 3-3′diaminobenzidine chromogen substrate, Haematoxylin counterstaining and specific antibodies raised against Cleaved Caspase-3 (D175, Cell Signaling Technology Inc., Danvers, Massachusetts, USA) and examined under light microscope (Olympus BX43). Cleaved Caspase-3 staining were quantified as ratio between positive cells and total cell number.

3.19. RNA extraction and quantification

RNA was extracted with QIAzol (Qiagen), following the manufacturer's instructions, and was subsequently quantified using Nanodrop Lite (Thermo Scientific).

3.20. Short RNA reverse transcription

The microRNAs were reverse transcribed using the miSCRIPT II RT kit (Qiagen) and following the company's instructions. For each sample, 1µg of RNA was reverse transcribed. Reverse transcription was performed with S1000 Thermal Cycler (Bio-Rad).

3.21. Long RNA reverse transcription

The RNA was reverse transcribed with the Quantitec kit according to the company's instructions; 1 µg of RNA was reverse transcribed for each sample. Reverse transcription was performed with S1000 Thermal Cycler (Bio-Rad).

3.22. Real-time PCR

Gene expression level was evaluated by Real-time PCR (primers listed in Table 2). Quantitative PCR was performed with SsoAdvanced Universal Supermix (Bio-Rad) on a CFX96 Real-Time System (Bio-Rad). A melting curve was performed after each PCR reaction to confirm the specificity of the primers. All reactions were performed in duplicate. Data were analysed using CFX Manager Software (Biorad).

3.23. Protein extraction

Melanoma cells (10^6) were resuspended in 70ul of lysis buffer (Tris HCl 50 mM, 1% TritonX100, 0.25% of NaDeoxicholate, PMSF 1mM, Orthovanadate 2mM, proteinase inhibitors cocktail). The mixture was incubated for 30 minutes on ice, then sonicated for 30 minutes, and finally centrifuged at 14000 *rpm* for 30 minutes at 4°C. The supernatant was then quantified using Bradford reagent and read at 590 nm.

3.24. Western blot

Proteins were detected by the following primary antibodies:

- anti-GAPDH (14C10, #2118, Cell Signaling Technology; rabbit monoclonal antibody, dilution 1:3000 in 3% milk in TBST);
- anti-LaminA/C (mab636, #MA3-1000, Thermo Fisher Scientific; mouse monoclonal antibody, dilution 1: 2000 in 3% milk in TBST);

- anti-PARP1 (F-2, #sc-8007, Santa Cruz Biotechnology; mouse monoclonal antibody, dilution 1:1000 in 3% milk in TBST);
- anti-p53 (DO-7, #M7001, Dako, mouse monoclonal antibody, dilution 1:1000).

3.25. Fractionation

6h after LNA transfection melanoma cells ($2X10^6$) were collected in PBS and were pelleted at 3500 *xg* for 5 minutes. Nuclear and cytoplasmic fractions were obtained by NE-PER™ Nuclear and Cytoplasmic Extraction Reagents (Thermo Fisher Scientific, ref. #78833), according to manufacturer's instructions. Finally, nuclear and cytoplasmic fractions were analysed by means WB as previously described.

3.26. RNA-sequencing

RNA-sequencing was performed in the lab of Dr. Paolo Malatesta in Genova. edgeR (Release 3.42.4) was used to perform comparisons between expression levels of genes. The genes with a log2 fold change (log2FC) higher than +0.4 or lower than −0.4 and an adjusted p-value of 0.05 were considered as differentially expressed.

3.27. Immunofluorescence

At the indicated time point, transfected cells were fixed with PFA4%. After 3 washes with PBS (5 minutes each one), they were permeabilized using Triton 0,2% (in PBS) at room temperature for 10 minutes. Once performing 3 washes with PBS, the cells were incubated with blocking (BSA 1% in PBS) at room temperature for 30 minutes. Then, the primary antibody (diluted in blocking) was added for 1h. After this incubation, 3 washes were performed followed by the incubation with secondary antibody (diluted in PBS). Finally, the cells were washed e the slides were analysed at the microscope. ImageJ was used for the quantitative analysis of fluorescence and the values were plotted in a bar graph.

The following primary antibody were utilized:

- anti-Myc-tag (71D10, #2278, Cell Signaling Technology; rabbit monoclonal antibody, dilution 1:200 in 1% BSA)
- anti-p53 (DO-7, M7001, Dako; mouse monoclonal antibody, dilution 1:100 in 1% BSA)

The following secondary antibody were used:

- red anti-mouse (A11032, Invitrogene; goat anti-mouse antibody, dilution 1:500 in PBS);
- red anti-rabbit (A11034, Invitrogene; goat anti-rabbit antibody, dilution 1:500 in PBS).

3.28. Statistical analysis

Unpaired t test and ANOVA test were used to analyse the data (GraphPad Prism, GraphPad Software Inc.). Values of $p<0.05$ were considered statistically significant (*$p<0.05$, **$p<0.01$, ***$p<0.001$, ****$p<0.0001$). The mean±SEM of three or more independent experiments is reported.

4. Results

4.1. The study of LNA-204 optimal dose and specificity

Once demonstrated that, in melanoma cells, if overexpressed miR-204 acts as oncosuppressor, to better define its role, I inhibited it by using the LNA-204, a custom oligonucleotide by Exiqon (Qiagen). In all biological and molecular assays two negative controls, LNA-CT and LNA-204-MM, were used. The LNA-CT has a nonspecific sequence, not complementary to any intracellular miRNA and, therefore, is used as a negative control. Regarding the LNA-204-MM, the wording MM means mismatch because the basis composition is identical to that of LNA-204, but the position of two nucleotides is switched (the 6th with the 10th and the 16th with the 18th), reason why the molecule loses its capacity to bind to the miRNA. In addition, LNA-211 is utilized to repress miR-211, since miR-204 and miR-211 are members of the same family. Below I reported the sequences of LNAs.

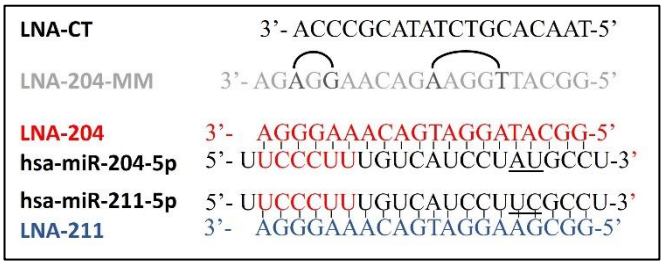

Figure 2. The sequence of LNAs and their respective miRNAs target.
LNA-CT (black), LNA-204-MM (grey), LNA-204 (red) and LNA-211 (blue). The color code is maintained in all subsequent graphs.
In LNA-204-MM sequence the two nucleotides whose position is switched are highlighted.
The sequences of hsa-miR-204-5p and hsa-miR-211-5p contain the seed region (red) and two discriminating bases (underline in black).

First of all, I established the concentration of LNA-204 able to completely block the activity of the endogenous miR-204. For this purpose, I used a sensor construct for miR-204: a strand complementary to that of mature miRNA (green) was cloned downstream of luciferase (firefly enzyme present in the species *Photinus piralis*) coding sequence (yellow) in pMIR vector. The endogenous miR-204 binds to the sensor sequence, inducing its cleavage, and consequently the luciferase signal decreases. The higher is the concentration of intracellular miR-204, the higher is the binding to sensor and its breakup, and the lower is the luciferase signal. On the contrary, in presence of the LNA-204, which inhibits the miRNA, a rescue in luciferase signal is observed.

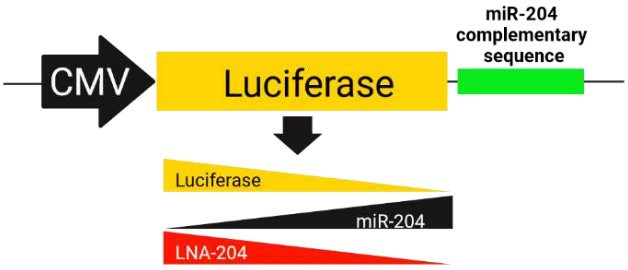

Figure 3. Schematic representation of sensor construct for miR-204.
As shown in the upper portion of picture, miR-204 complementary sequence (green) is located downstream of reporter gene (yellow) under the regulation of CMV promoter (black).
In the lower portion of picture, the expected intensity of luciferase signal (yellow) is represented in relation to the concentration of LNA-204 (red) and miR-204 (black).

In order to achieve my aim, I performed the luciferase assay in A375 cells. This assay exploits the bioluminescence reaction during which light is produced through the oxidation of a pigment, luciferin, by luciferase. Transfecting a fixed amount of sensor plasmid and a plasmid expressing Renilla luciferase (pTK) used as a normalizer, I tested different doses of miR-204 inhibitor (5-120 nM) and I considered as baseline (maximal miR-204 activity) the cells co-transfected with sensor plus 120 nM of LNA-CT (black bar). At 24h I read the samples with the luminometer and, as shown in the bar graph (Figure 4), following the co-transfection of LNA-204, the luciferase activity increased in according with the increment of LNA concentration (dose dependent manner), reaching a plateau at 60nM. Therefore, the results suggested that 60nM of LNA-204 is sufficient to fully inhibit the endogenous miRNA.

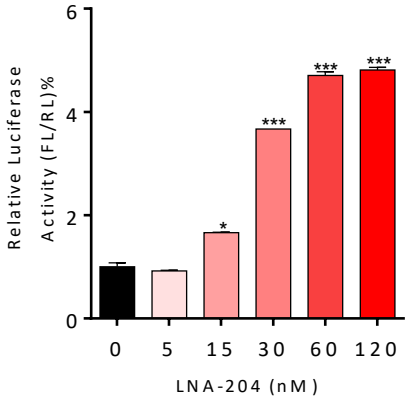

Figure 4. Luciferase assay testing increasing doses of LNA-204 to establish the dose able to fully block the activity of endogenous miR-204.
The bar graph shows the relative luciferase activity at 24h from the transfection of 120nM LNA-CT (black bar) and indicated doses of LNA-204 (red bars) in A375 cells. The luciferase signal gradually increases (different red colour intensity) as LNA-204 concentration increases, reaching a plateau at 60nM: 60nM is sufficient to completely inhibit the endogenous miRNA. The mean ± SEM of 2 independent experiments is reported. *p<0.05; ***p<0.001.

Then, exploiting the sensor construct, I investigated the specificity of LNA molecules. I performed the luciferase experiment in HCT116 Dicer-/- cells in which there is not the expression of mature miRNAs due to the lack of Dicer complex and, hence, it is possible to exogenously control miR-204 levels. I chose this cell line to transfect the miR-204 sensor together with si-CT or 204-mimic in order to overexpress miR-204, as well as 60nM of LNA-CT, LNA-204 or LNA-204-MM. The results plotted in the graph (Figure 5) revealed that only LNA-204 is able to rescue the luciferase signal, while LNA-204 MM is not. Thus, I demonstrated that, contrary to LNA-204, LNA-204-MM is not capable to bind to miR-204 and to repress it.

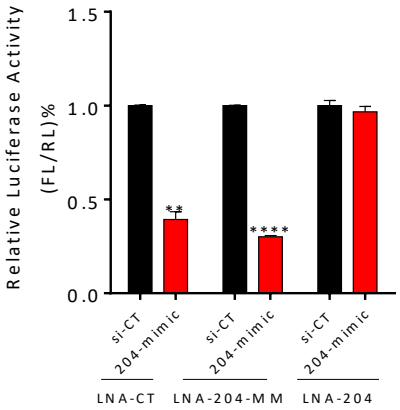

Figure 5. LNA-204 is able to rescue the luciferase signal due to miR-204 overexpression (204-mimic).
The graph shows the results of luciferase assay at 24h from the co-transfection of si-CT (black) or 204-mimic (red) and LNA CT, LNA-204-MM or LNA-204 in HCT116 Dicer -/-. miR-204 overexpression causes the reduction in luciferase activity: LNA-204 is able to rescue the luciferase signal, while LNA-204-MM has no effect. The mean ± SEM of 3 independent experiments is reported. **p<0.01; ****p<0.0001.

4.2. The effects of miR-204 inhibition in cell cultures

4.2.1. LNA-204 induces caspase-dependent apoptosis

Once established the dose of LNA-204 to use, with the aim to study the biological effects of miR-204 inhibition *in vitro*, I transfected A375 cells with 60nM of indicated LNAs. As evidenced, the transfection of LNA-204, but not of LNA-204-MM, causes a significant decrease in cell proliferation (Figure 6), cell viability (Figure 7) and colony forming capability (Figure 8).

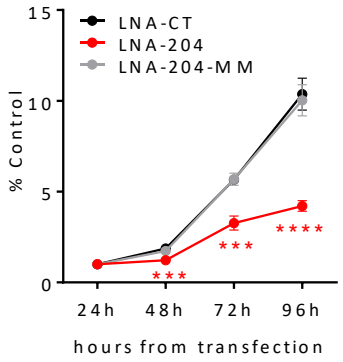

Figure 6. The effect of LNA-204 on cell proliferation.
The results of cell proliferation assay at 24h, 48, 72, and 96h from the transfection of LNA-CT (black), LNA-204-MM (grey) or LNA-204 (red) are plotted. The mean ± SEM of 3 independent experiments is reported. ***p<0.001; ****p<0.0001.

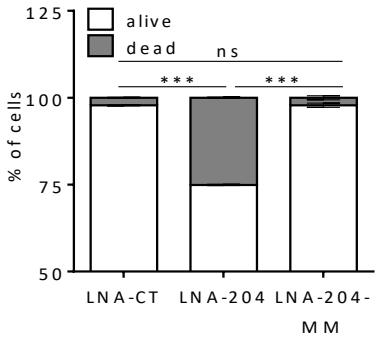

Figure 7. The effect of LNA-204 on cell viability.
The graph reports the percentage of alive (white) and dead (grey) cells at 24h from the transfection of LNA-CT, LNA-204-MM or LNA-204. The mean ± SEM of 2 independent experiments is reported. ***p<0.001.

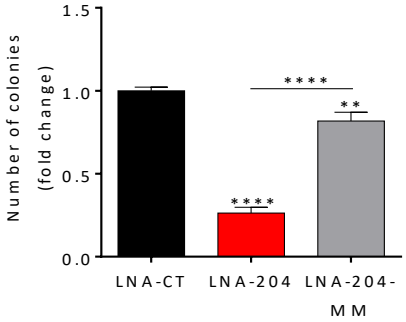

Figure 8. The effect of LNA-204 on colony forming capability.
The graph shows the number of colonies after 8 days from the transfection of LNA-CT (black), LNA-204-MM (grey) or LNA-204 (red). The mean ± SEM of 3 independent experiments is reported. **p<0.01; ****p<0.0001.

This statistically significative decrease in cell proliferation, cell viability and number of colonies is due to increased apoptosis, as suggested by the cell cycle analysis, in particular the increased percentage of cells in sub-G1 phase (Figure 9). Actually, the percentage of cells in sub-G1 progressively increases over time between 6h and 24h after miR-204 inhibition (Figure 10).

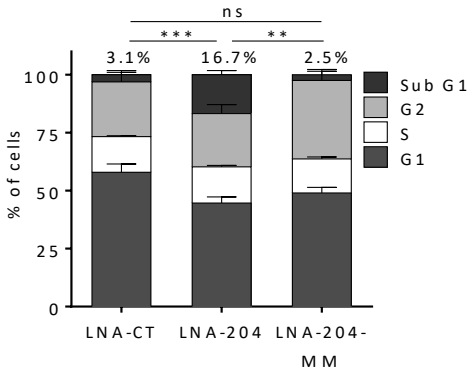

Figure 9. LNA-204 causes an accumulation of cells in sub-G1 phase of cell cycle.
The figure shows the results of cell cycle analysis performed at 24h from the transfection of LNA-CT, LNA-204-MM or LNA-204. Percentage of cells in sub-G1 phase is reported in the graph as well as statistics relative to this group of cells. The mean ± SEM of 4 independent experiments is reported. **p<0.01; ***p<0.001.

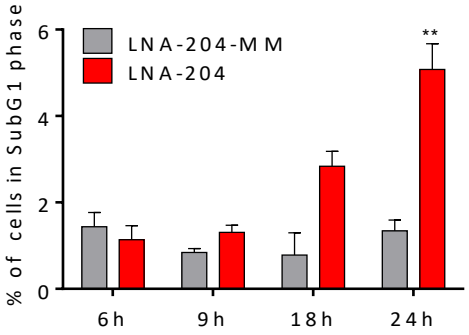

Figure 10. The gradual increment of cells in sub-G1 phase due to miR-204 inhibition.
The graph shows the percentage of cells in sub-G1 phase between 6h and 24h from the transfection of LNA-204-MM (grey) LNA-204 (red). The mean ± SEM of 3 independent experiments is reported. **p<0.01.

In order to confirm that LNA-204 induces apoptosis, I transfected A375 cells with LNA-CT, LNA-204-MM or LNA-204, and at 18h, 24h and 48h post transfection I performed the Annexin assay (protocol in Material and Methods). This assay allows to discriminate between alive cells and early/late apoptotic cells by exploiting Annexin-FITC and PI stainings. As you can see from the curve trend, the percentage of Annexin-V positive cells profoundly increases after the transfection of LNA-204 (Figure 11).

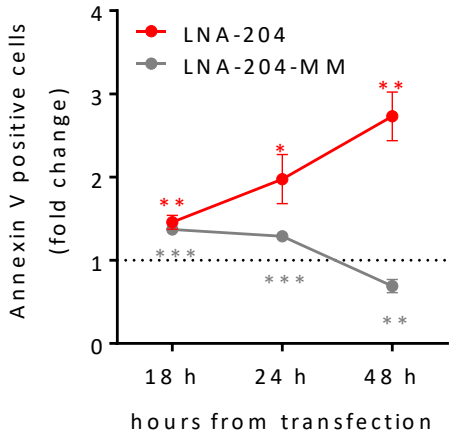

Figure 11. LNA-204 induces the increment in apoptosis.
The curve shows the percentage of Annexin V positive cells at 18h, 24h and 48h from the transfection of LNA-204-MM (grey) or LNA-204 (red). A significative increment in apoptosis is observed after the inhibition of miR-204. The mean ± SEM of 4 independent experiments is reported. *p<0.05; **p<0.01; ***p<0.001.

In order to understand which pathway mediates the apoptosis, I investigated both intrinsic and extrinsic apoptotic pathways. The intrinsic pathway is activated by intracellular signals and the key regulator is caspase-9, while the extrinsic pathway is activated by extracellular stimuli and it is triggered by caspase-8. Caspase-8 and caspase-9 represent the initiator caspases and have a common target, caspase 3/7, defined as effector. For my aim, I performed the caspase

assay which consists in quantifying the relative activity of Caspases 3/7, 8 and 9. I used a kit, specific for each molecule to analyse, that provides a proluminescent caspase substrate and a thermostable luciferase. After cell lysis, the substrate is cleaved by the caspase. The cleavage releases a substance that is consumed by luciferase, generating a luminescent signal that is proportional to the activity of the caspase. As per protocol, I transfected the cells with LNA NC, LNA-204 or LNA-204-MM and, 9h after the transfection, following the addition of the reagent and a fixed incubation period, I read the samples with the luminometer. As can be seen in the graph below (Figure 12 *left*), no change is detected in the level of the examined caspases. Instead, at 18h as well as at 24h, following LNA-204 transfection, all caspases activity significantly increased compared to the negative control (Figure 12 *middle and right*). The increment in the activity of caspase-3 (effector) is very evident since it represents the common target of both caspase-8 and caspase-9. However, the most interesting result is that the activity of both initiator caspases increased. The greater level of caspase-9 activity is due to the fact that it is more sensitive to the reagent. Therefore, based on the obtained results, I can conclude that there is not a prevalent apoptotic pathway, but both the intrinsic and the extrinsic are induced.

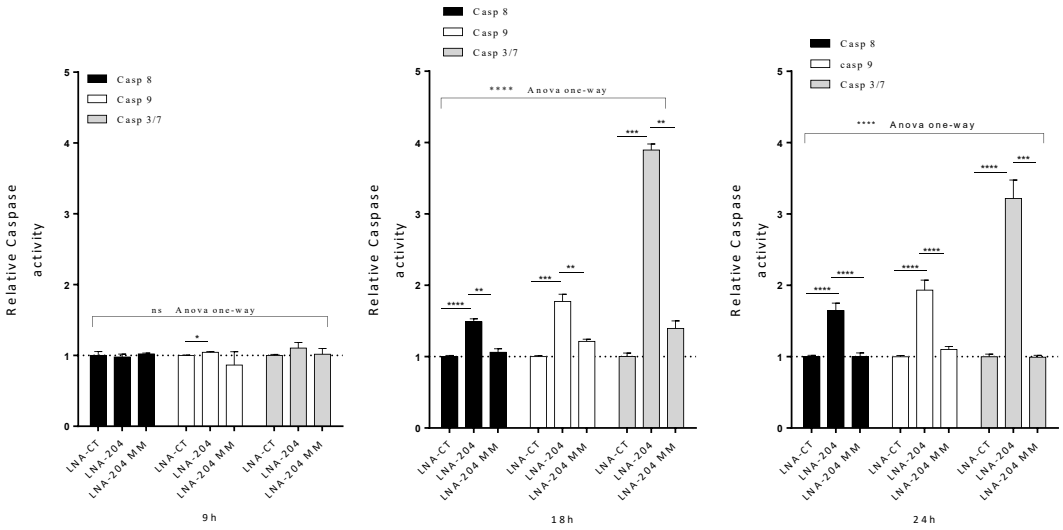

Figure 12. Both intrinsic and extrinsic pathways are activated by LNA-204.
The activity of caspase 3/7 (grey), caspase-8 (black) and caspase-9 (white) was evaluated at 9, 18 and 24h after the transfection of the LNA-CT, LNA-204-MM or LNA-204. At 18h and 24h caspases 3/7, 8 and 9 are all activated by LNA-204. The mean ± SEM of 3 independent experiments is reported. *p<0.05; **p<0.01; ***p<0.001; ****p<0.0001.

In literature it's known that Caspase 3/7, once activated, induces the cleavage of PARP1 protein at the nuclear level. For this reason, as further confirmation of the apoptotic cell death, I measured PARP1 protein level. The results, that confirm the expectation, are reported in the WB analysis (Figure 13): in LNA-204 sample is present a second band which represents the cleaved protein.

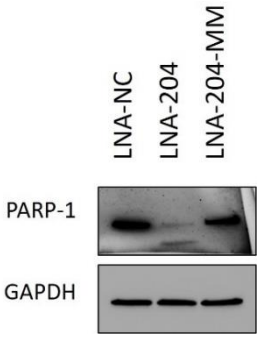

Figure 13. The cleavage of PARP1 protein by activated Caspase 3/7 after the transfection of LNA-204.
Cleaved PARP1 protein levels are measured at 24h after the transfection of LNA-CT (line 1), LNA-204 (line 2) or LNA-204-MM (line 3). In line 2 (LNA-204 sample) the cleaved PARP1 protein was detected. A representative of 2 independent experiments is reported.

4.2.2. Apoptosis induced by LNA-204 is specifically due to miR-204 inhibition

In all experiments described, I compared LNA-204 with LNA-NC and LNA-204-MM. As previously mentioned, the sequence of LNA-204-MM is the same as that of LNA-204, except for two bases whose position is switched, and this feature abrogates the ability of the molecule to bind to miR-204. Actually, the activity of LNA-204-MM is comparable to that of LNA-CT rather than LNA-204. This suggested that the biological consequences correlated with LNA-204 are due to the inhibition of miR-204, and not to toxic, off-targets effects. However, to ensure that unwanted effects are excluded, I transfected melanoma cells with increasing amounts (15-120 nM) of LNA-CT and LNA-204 and estimated cell viability. At higher concentrations, the vitality is affected by LNA-CT, which indicated the insurgence of toxic effects, while in the 15-60nM range only LNA-204 caused a decrease in cell viability and the most interesting thing is that the reduction is dose-dependent (Figure 14).

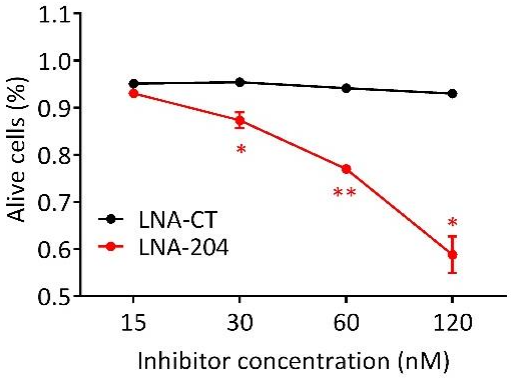

Figure 14. Evaluation of LNA-204 toxic effects in the 15-120nM range.
The curve represents cell viability trend in A375 cells transfected with increasing amounts of LNA-CT (black line) or LNA-204 (red line). The decrease in cell viability caused by LNA-204 is dose-dependent. The mean±SEM of 3 independent experiments is reported. *p<0.05; **p<0.01.

To demonstrate that, like the reduction of cell viability, the apoptosis is also induced by LNA-204 in a dose-dependent manner, I used A375 sgRNA miR-204 cells, in which the endogenous level of miR-204 is reduced (approximately 70%) compared to control A375 sgRNA AVV1 cells by means of CRISPR/Cas9 technology (Figure 15) [20].

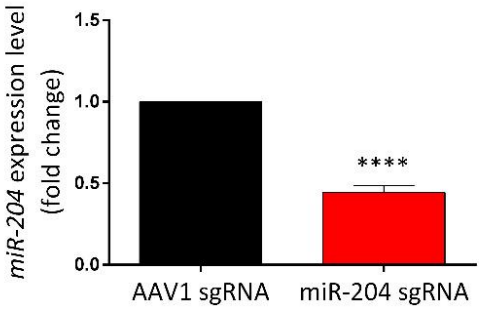

Figure 15. Reduction of endogenous miR-204 levels by means of CRISPR/Cas9 technology.
miR-204 expression level was quantified by qRT-PCR in A375 sgRNA miR-204 (red) compared to A375 sgRNA AVV1 (black). The mean ± SEM of 3 independent experiments is reported. ****p<0.0001.

Since in A375 sgRNA miR-204 cells the amount of intracellular miR-204 is lower than in the control (A375 sgRNA AVV1 cells), I expect that a minor dose of LNA-204 is needed to totally inhibit the miRNA. To demonstrate this, I performed the luciferase assay with the sensor construct mentioned above. I transfected A375 sgRNA miR-204 and A375 sgRNA AVV1 cells with increasing doses of LNA-204 (5, 15, 30, 60nM) and a single dose of LNA-NC (60 nM), in addition to the sensor plasmid and the normalizer (pTK). I considered as baseline the signal obtained for the sample transfected with the LNA-NC. In the samples transfected with LNA-204, the endogenous miR-204, being inhibited, cannot repress the reporter expression. As miR-204 inhibition is proportional to the dose of LNA used, I expect the luciferase activity to progressively increase as the dose of LNA increases until a plateau is reached which indicates that the inhibition of the endogenous miRNA is total. The results are represented with a dose-response curve (Figure 16): in the control line (A375 sgRNA AVV1) the luciferase signal is maximum in cells transfected with 30nM of LNA-204, while in A375 sgRNA miR-204 a lower dose of LNA-204 (15nM) is sufficient, in according with the presence of a lower quantity of endogenous miRNA. Ultimately, the data indicated confirmed that A375 sgRNA miR-204 contains less miR-204 than A375 sgRNA AVV1, as a lower concentration of LNA-204 is necessary to inhibit it.

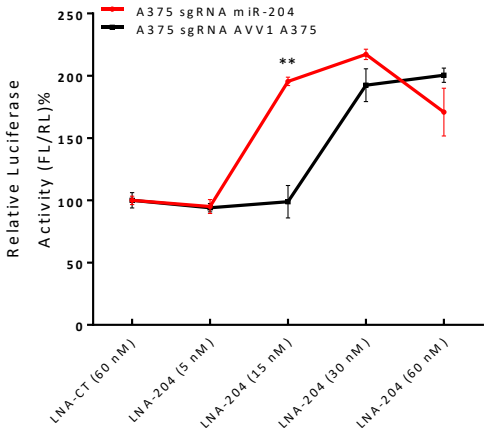

Figure 16. A lower dose of LNA-204 is necessary to fully inhibit the endogenous miR-204 in A375 sgRNA miR-204 compared to A375 sgRNA AVV1.
The graph shows the results of luciferase assay performed at 24h after the transfection of 60nM LNA-CT or indicated dose of LNA-204 in A375 sgRNA miR-204 (red curve) and A375 sgRNA AVV1 (black curve). 15nM is the dose able to completely inhibit the endogenous miR-204 in A375 sgRNA miR-204 compared to 30nM needed to have similar effect in A375 sgRNA AVV1. The mean ± SEM of 4 independent experiments is reported. **p<0.01.

Once established that 15nM of LNA-204 is sufficient to fully block the activity of the endogenous miR-204 in A375 sgRNA miR-204 but not in A375 sgRNA AVV1 cells, I performed the Annexin assay. In particular, I transfected the two cell lines with 15nM LNA-204 and 48h later, I read the samples by facs. From the graph (Figure 17), you can see that, subsequent the transfection with LNA-204, in both A375 sgRNA miR-204 and A375 sgRNA AVV1 there is an increase in the percentage of apoptotic cells which is statistically significant compared to the corresponding control (LNA-NC). However, the most relevant result is that, transfected at 15nM, LNA-204 produces a stronger apoptotic effect in A375 sgRNA miR-204 rather than in control cells and this is consistent with the total inhibition of intracellular miR-204.

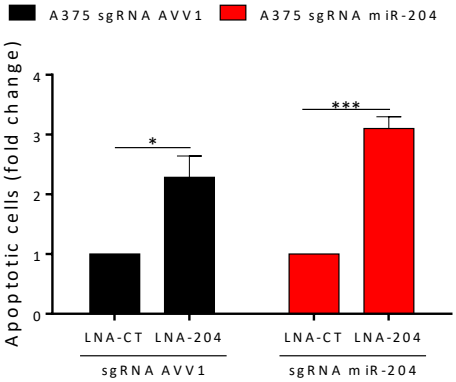

Figure 17. The quantification of apoptotic cells in A375 sgRNA miR-204 and in A375 sgRNA AVV1 after the transfection of 15nM LNA-204.
The apoptosis was measured by means Annexin V assay at 48h after the transfection of 15nM of LNA-CT or LNA-204 in A375 sgRNA AVV1 (black) and A375 sgRNA miR-204 (red). The transfected dose of LNA-204 has a stronger apoptotic effect in A375 sgRNA miR-204 compared to A375 sgRNA AVV1. The mean ± SEM of 3 independent experiments is reported. *p<0.05; ***p<0.001.

In addition, I tested whether 204-mimic, exogenously supplied to overexpress the endogenous miR-204, is able to rescue the proapoptotic effect of the LNA. I transfected A375 cells with the combinations of LNAs plus siRNA mimics specified in Figure 18a and after 24h I performed the protocol of Annexin V/PI stainings. During facs analysis cell populations are graphically divided into 4 quadrants: the lower left quadrant contains alive cells, the lower right quadrant the early apoptotic cells, the upper right quadrant the late apoptotic cells and the upper left quadrant the necrotic cells. Then, I analysed the data and reported the total percentage of alive cells and dead cells in a graph bar (Figure 18b). Co-transfecting LNA-204 and 204-mimic (third bar), I observed a rescue of apoptosis compared to the transfection of LNA-204 plus the control mimic (second bar). These results indicate that LNA-204 induced apoptosis is specifically due to miR-204 inhibition and not to a toxic, aspecific effect. In my next experiments I used 204-mimic as positive control for miR-204 inhibition rescue.

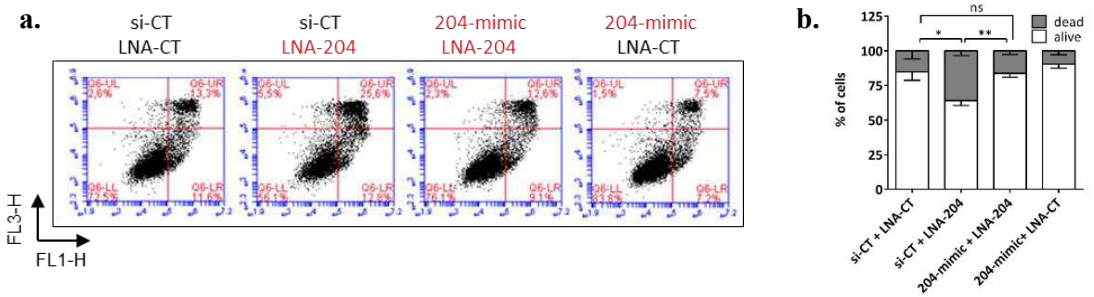

Figure 18. 204-mimic is able to rescue the apoptosis induced by LNA-204.
(a) Graphic representation of the percentage of alive cells (lower left quadrant), early apoptotic cells (lower right quadrant), late apoptotic cells (upper right quadrant) and necrotic cells (upper left quadrant) at 24h from the transfection of the indicated combinations of LNA-CT or LNA-204 plus si-CT or 204-mimic. (b) The total percentage of alive cells (white) and dead (grey) cells is reported for each experimental condition. The mean ± SEM of 3 independent experiments is reported. *p<0.05; **p<0.01.

4.2.3. Comparison between LNA-204 and LNA-211 effects

Given that miR-204 and miR-211 belong to the same family and target the same genes when overexpressed, I investigated whether the proapoptotic effects are specifically due to miR-204 inhibition or miR-211 as well by using the sensor construct for miR-204 described in paragraph 4.1. In Figure 19 a schematic representation of the interactions between the sensor construct for miR-204 and LNAs is shown.

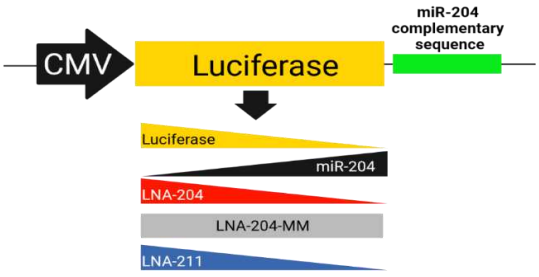

Figure 19. A representation of the interactions between the sensor construct for miR-204 and LNA-204-MM (grey), LNA-204 (red) and LNA-211 (blue).
The picture is described in Figure 3. In addition, although the construct sequence is perfectly complementary to miR-204, in conditions of overexpression, it is also recognized and bound by miR-211 and, despite, the pairing is imperfect, a reduction in the luciferase signal is observed.

First of all, I performed the luciferase assay to investigate the affinity of LNAs for miR-204. Particularly, I co-transfected the sensor plus 60nM of LNA-CT, LNA-204 or LNA-211 in A375 cells which endogenously express miR-204, but not miR-211. A rescue in luciferase activity was observed only in presence of LNA-204, not in presence of LNA-211. The data (Figure 20) indicated that, although miR-204 and miR-211 belong to the same family, miR-204 is specifically inhibited by LNA-204, while LNA-211 has no effect.

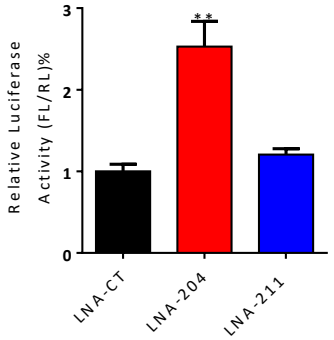

Figure 20. Luciferase assay to investigate the effect of LNA-204 and LNA-211 on the endogenous miR-204.
The graph reports the results of luciferase assay at 24h from the transfection of 60nM LNA-CT (black), LNA-204 (red) or LNA-211 (blue) in A375 cells. An increment in luciferase signal is observed only after the transfection of LNA-204, but not of LNA-211: the endogenous miRNA is specifically inhibited by LNA-204. The mean ± SEM of 4 independent experiments is reported. **p<0.01.

Then, I repeated the assay in HCT116 Dicer -/- in order to check that the binding of LNA-204 and LNA-211 to their intended miRNA is specific. In this case, I transfected si-CT, 204-mimic or 211-mimic with LNA-CT, LNA-204 or LNA-211. As already reported in Figure 5, by overexpressing the endogenous miR-204 (204-mimic), I observed an increase in luciferase signal only after LNA-204 transfection, while the LNA-211 is specifically able to rescue the luciferase signal of miR-211 overexpression (211-mimic) (Figure 21). In conclusion, I demonstrated that LNA-204 and LNA-211 are specific inhibitors and they selectively block the activity of miR-204 and miR-211 respectively.

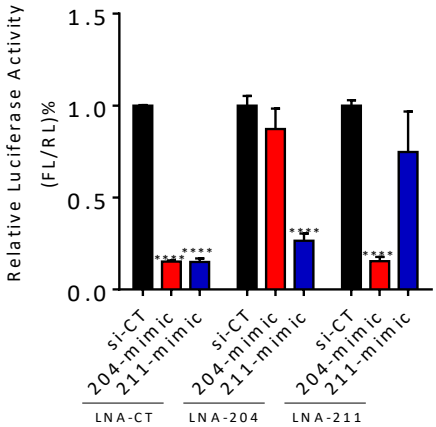

Figure 21. The ability of LNA-204, but not of LNA-211, to rescue the luciferase signal due to exogenous miR-204 overexpression.
The bar graph reports the results of luciferase assay performed at 24h from the co-transfection of si-CT (black), 204-mimic (red) or 211-mimic (blue) and LNA-CT, LNA-204 or LNA-211 in HCT116 Dicer -/- . The luciferase signal is specifically rescued by LNA-204, but not LNA-211. The mean ± SEM of 2 independent experiments is reported. ****p<0.0001.

Once validated the specificity of LNA-204 and LNA-211, I transfected 60nM of both inhibitors in 501Mel cells which express miR-204 and miR-211 and I found that cell proliferation (Figure 22) and colony formation (Figure 23) are impaired only by miR-204 inhibition, while miR-211 inhibition does not affect them.

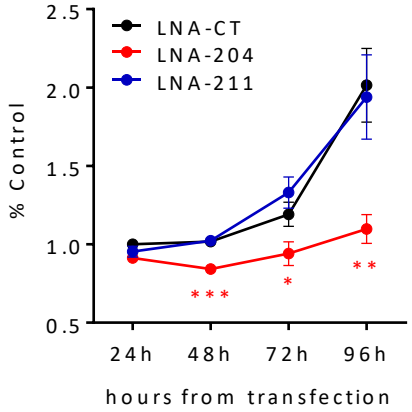

Figure 22. Comparison between the effect of LNA-204 and the effect of LNA-211 on cell proliferation.
The graph shows the results of cell proliferation assay at 24h, 48, 72, and 96h from the transfection of LNA-CT (black), LNA-204 (red) or LNA-211 (blue). A strong decrease in cell proliferation is observed after the transfection of LNA-204, while LNA-211 has not effect. The mean ± SEM of 3 independent experiments is reported. *p<0.05; **p<0.01; ***p<0.001.

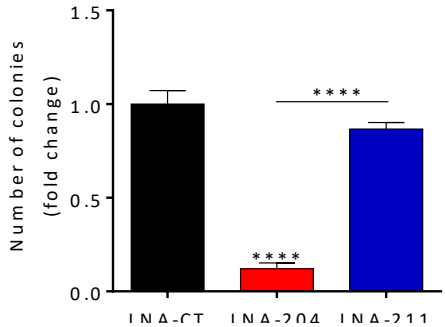

Figure 23. Comparison between the effect of LNA-204 and the effect of LNA-211 on colony forming capability.
The graph shows the number of colonies (fold change) after 8 days from the transfection of LNA-CT (black), LNA-204 (red) or LNA-211 (blue). A lower number of colonies is plotted after the transfection of LNA-204, but not of LNA-211. The mean ± SEM of 3 independent experiments is reported. ****p<0.0001.

Moreover, in order to evaluate if the apoptosis induced by LNA-204 is a general phenomenon, at 24h after the transfection of standard dose of LNAs, I performed the Annexin-V-FITC/PI staining on a large number of melanoma cell lines. Among these, some carry the $BRAF^{V600E}$ mutation (A375, 501Mel, C32, SK-Mel5, UACC62, COLO800, M14, A2058), some are their vemurafenib-resistant derivatives previously generated in our lab (A375 C2, A375 P2, 501Mel P1) [20] and some are wtBRAF cell lines (MeWo). I transfected LNA-204 and LNA-211 in all cell lines except A375 parental cell line and its resistant derivatives, C32 and COLO800 that were not transfected with LNA-211 because they do not express miR-211.

As shown in Figure 24, the inhibition of endogenous miR-204, not of miR-211, causes a profound increase of apoptosis in all cell lines, independently of BRAF mutational status. Interestingly, the increased apoptosis observed in melanoma clones (A375 C2 clone) and cell populations (A375 P2 population and 501 Mel P1 population) resistant to vemurafenib treatment suggests that the proapoptotic effect of LNA-204 menages to evade drug resistance mechanisms. In conclusion, I proved that apoptosis is a specific biological effect associated with miR-204 inhibition, but not of miR-211 inhibition.

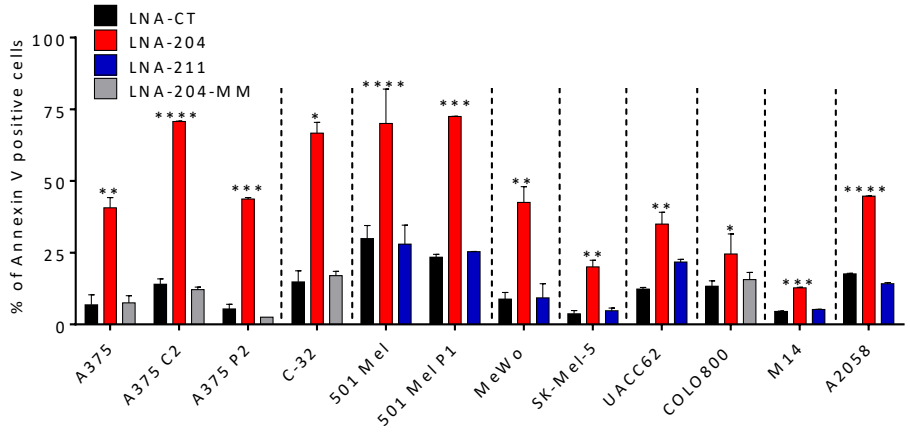

Figure 24. The apoptosis LNA-204 induced is specifically due to the inhibition of miR-204 and it evades drug resistance mechanisms.
The apoptotic cells are detected by means the Annexin-V-FITC/PI staining at 24h after the transfection of LNA-CT (black), LNA-204-MM (grey), LNA-204 (red) or LNA-211 (blue) on melanoma cell lines. An increase in percentage of Annexin-V-FITC/PI is specifically induced by LNA-204, but not by LNA-211. The mean ± SEM of 3 independent experiments is reported. *p<0.05; **p<0.01; ***p<0.001; ****p<0.0001.

4.3. LNA-204 inhibits tumor growth in *in vivo* melanoma models

In order to reinforce the pro-apoptotic activity of LNA-204 in melanoma, I studied the effect of miR-204 inhibition in *in vivo* models (zebrafish and nude mouse) using the xenograft technique, as well as in a genetically engineered mouse model.

4.3.1. Antiproliferative effect of LNA-204 in zebrafish embryos

The first model system in which we performed *in vivo* experiments was zebrafish. We transfected A375-mCherry cells with 60nM LNA-CT or LNA-204 and 6h after the transfection we injected the cells into the yolk sac of 48 post fertilization zebrafish embryos. Once xenografted, we measured the relative tumor area at 3.5h (baseline) and at 48h post-graft. In Figure 25 we reported representative pictures of embryos taken at 3.5h and 48h post-graft

(scale bar: 100um), while in Figure 26 we plotted the results relative to the measurement of area of red cell masses. As shown in the bar graph, at 48h the area of tumor mass derived from cells transfected with LNA-204 is reduced compared to that of negative control. The data suggested that LNA-204 inhibits the tumor growth also *in vivo* as widely demonstrated in cultured cells.

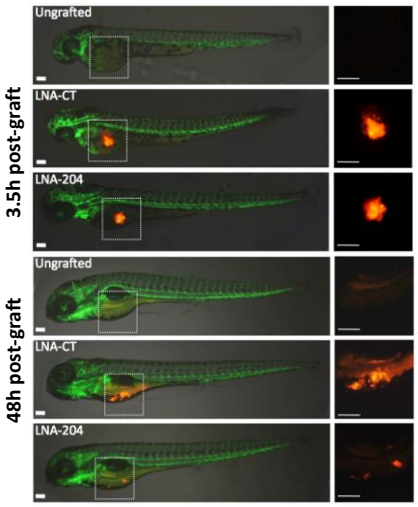

Figure 25. Representative pictures of zebrafish embryos taken at 3.5h and 48h post-graft.
At 6h from transfection A375-mCherry cells (red signal) transfected with 60nM LNA-CT or LNA-204 are injected in yolk sac (highlighted in pictures). Scale bar: 100um.

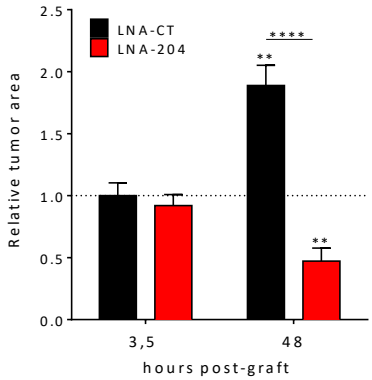

Figure 26. LNA-204 inhibits tumor growth in zebrafish embryos.
The bar graph represents the relative area of red cell masses at 3.5h post graft (baseline) and at 48h post graft (pictures in Figure 25). As shown, at 48h the area of tumor derived from A375-mCherry cells transfected with LNA-204 (red) is reduced compared to negative control (black). The mean ± SEM of 3 independent injections is reported. **p<0.01; ****p<0.0001.

In addition, we repeated the xenograft of 501Mel cells transfected with LNA-CT, LNA-204, LNA-204-MM or LNA-211 in zebrafish embryos and these experiments confirmed that the antiproliferative effect is associated only to LNA-204, not to LNA-204-MM and LNA-211 (Figure 27).

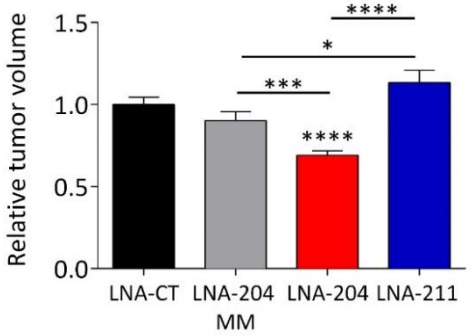

Figure 27. Comparison between the effect of LNA-204 and the effect of LNA-211 on tumor growth in zebrafish embryos.
The figure shows the relative volume of tumors derived from 501Mel transfected with 60nM of LNA-CT (black), LNA-204-MM (grey), LNA-204 (red) or LNA-211 (blue) and injected in zebrafish embryos. A significant decrease in tumor volume is observed with the transfection of LNA-204, but not LNA-211. The mean ± SEM of 3 independent injections is reported. *p<0.05; ***p<0.001; ****p<0.0001.

4.3.2. Antiproliferative effect of LNA-204 in nude mice

We used the nude mouse as a second model to investigate the proapoptotic activity of LNA-204 *in vivo* taking advantage of the fact that the human sequence of miR-204 is identical to the mouse sequence (Figure 28).

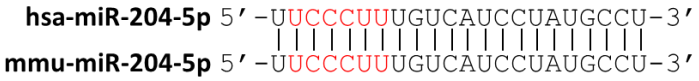

Figure 28. Human and mouse miR-204 sequence (5'→3').
The alignment between human (upper) and mouse (lower) miR-204 shows that the 2 sequences are identical. The seed region is reported in red.

In this case, we transfected A375 cells with LNA-CT and LNA-204 and, after 48h from the transfection, we subcutaneously injected the cells in the flank of nude mice (n = 12 per experimental condition) and measured the tumor volume by caliper twice per week for up to 50 days. As reported in the curve (Figure 29), during the follow-up period, A375 transfected with LNA-204 did not form measurable tumors.

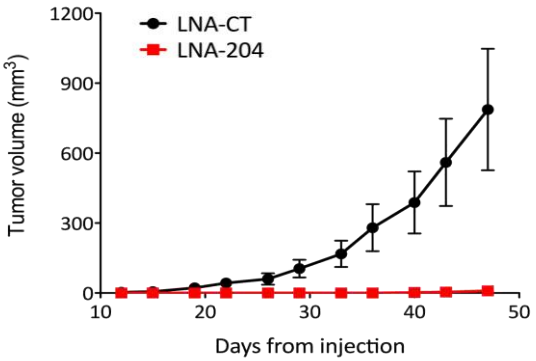

Figure 29. Antiproliferative effect of LNA-204 in mice: it inhibits tumor growth leading to a decrease in tumor volume.
The curve indicates the volume of tumors formed by A375 transfected with LNA-CT (black) or LNA-204 (red) measured twice per week for up to 50 days. Cells transfected with LNA-204 did not form measurable tumors compared to control. N=12 per experimental condition.

At the end of 50 days, we excised the tumors and measured their weight. We found only 1 weighable mass derived from cells transfected with LNA-204 and it had a significantly lower weight than the weight of tumors formed by cells transfected with LNA-CT (Figure 30). Crucially, the reduction in tumor volume and tumor weight can be ascribed to the ability of LNA-204 to prevent the proliferation of mouse melanoma cells, as suggested by the decrease in proliferation of B16F10 mouse melanoma cells induced by LNA-204, but not LNA-204-MM and LNA-211 (Figure 31).

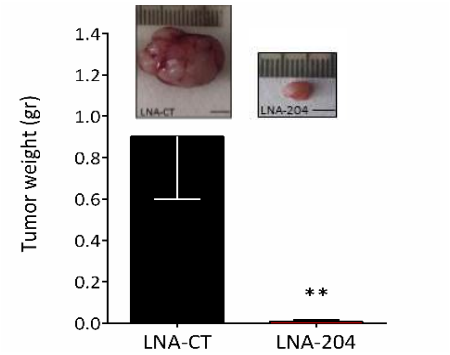

Figure 30. Antiproliferative effect of LNA-204 in mice: it inhibits tumor growth leading to a decrease in tumor weight. The pictures show a representative tumor formed by A375 cells transfected with LNA-CT, as well as the only weighable tumor formed by A375 cells transfected with LNA-204 after a follow-up period (50 days). **p<0.01.

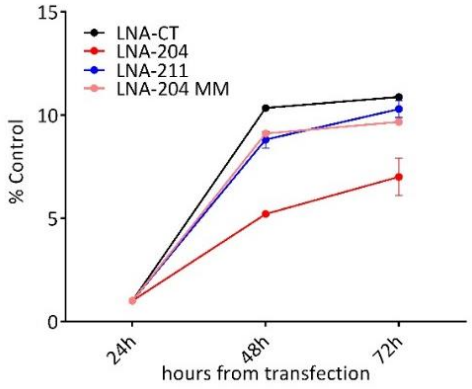

Figure 31. Effect of LNA-204 and LNA-211 on proliferation in B16F10 mouse melanoma cells. The curve reports the percentage of proliferation in B16F10 mouse melanoma cells at 24h,48h and 72h after the transfection of LNA-CT (black), LNA-204-MM (grey), LNA-204 (red) or LNA-211 (blue). LNA-204 causes a decrease in cell proliferation, while LNA-211 does not affect it. The mean ± SEM of 3 independent experiments is reported.

4.3.3. Antiproliferative effects of LNA-204 in the Braf/Pten genetically engineered mouse model of melanoma

In order to evaluate the efficacy of LNA-204 in therapeutic settings, i.e. on a preexisting melanoma tumors, we utilized the Tyr::CreER+,BrafCA/+,Ptenlox/lox (Braf/Pten) genetically engineered mouse model of melanoma. Particularly, we spread the back of 6 week-old mice with 4-HT that induce two genetic mutations, the switch from wt to BrafV600E and the loss of Pten, causing melanoma development. Within 4 weeks, primary melanomas appear with a volume of 50-100mm^3. At this point, once complexed with Lipofectamine 2000, we injected intratumorally 1nmole of LNA-CT or LNA-204 and we performed 1 injection every 4 days, for a total of 4 injections (Figure 32).

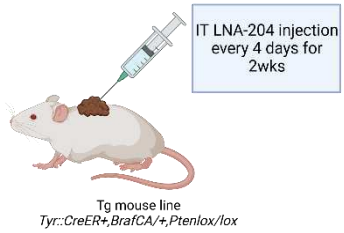

Figure 32. Experimental protocol used in Braf/Pten genetically engineered mouse model of melanoma.
4-HT is spread on the back of the mouse to induce the development of melanoma. After the appearance of the tumor, LNA-CT or LNA-204 is intratumorally injected every 4 days for 2 weeks (4 injections in total).

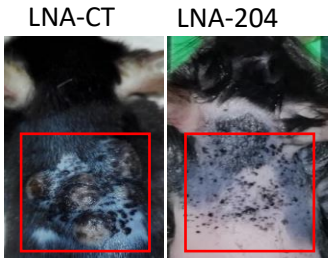

Within 3 days after the last intra-tumoral injection, we photographed primary tumors (Figure 33) and then excised them to calculate their weight. As shown in Figure 34 the tumors treated with LNA-204 shown a weight significantly lower than those treated with LNA-CT.

Figure 33. Antiproliferative effect of LNA-204 in Braf/Pten genetically engineered mouse model of melanoma.
The pictures depict primary tumor after intra-tumoral within 3 days after the last injection of LNA-CT or LNA-204. As shown, the size of primary tumor decreases after the intra-tumoral injection of LNA-204 compared to control.

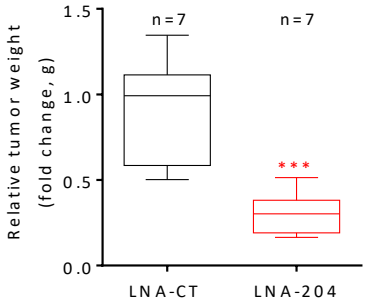

Figure 34. LNA-204 induces a decrease in tumor weight on Braf/Pten genetically engineered mouse model of melanoma.
The bar graph indicates the relative weight of excised tumors treated with LNA-CT (black) or LNA-204 (red) in Braf/Pten genetically engineered mouse model of melanoma. The weight of tumors treated with LNA-204 is lower than the tumors treated with LNA-CT. The mean ± SEM of 3 independent injections is reported. ***p<0.001.

Additionally, we performed haematoxylin and eosin staining. Thanks to H&E analysis we found that the tumors treated with LNA-204 are much thinner than LNA-CT treated ones (Figure 35), so this confirms their smaller size as shown in previous figure.

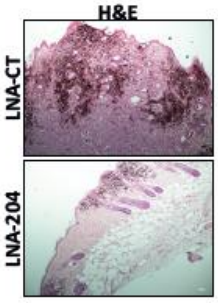

Figure 35. H&E analysis confirms the antitumor activity of LNA-204.
Haematoxylin and eosin staining reveal that tumors treated with LNA-204 are thinner than LNA-CT treated ones as shown in representative pictures.

In order to identify the cause of the decrease in tumor size/weight, we performed the immunohistochemistry experiment in which we used Cleaved Caspase-3 (CC3) and TUNEL staining, as markers of apoptosis, and Ki67 staining, as marker of proliferation. The analysis of samples (illustrative images in Figure 36) revealed that the tumors treated with LNA-204 are characterized by a higher numbers of Cleaved Caspase-3 positive cells (apoptotic cells) and a stronger signal of Ki67 staining. Therefore, IHC analysis indicate that LNA-204 causes the reduction in tumor size/weight inducing apoptosis and suppressing proliferation.

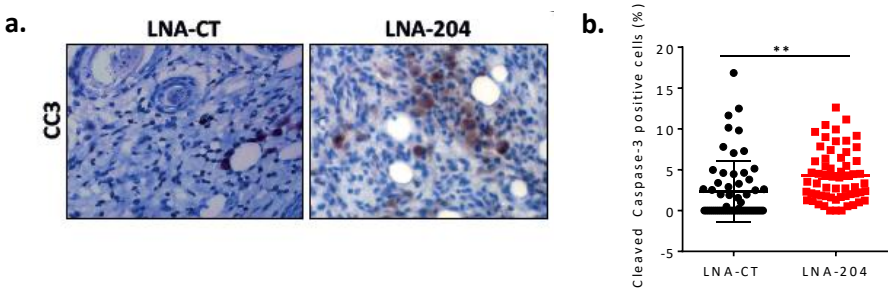

Figure 36. LNA-204 causes a reduction in tumor size/weight inducing apoptosis.
(a) Illustrative images of IHC analyses performed on tumors treated with LNA-CT or LNA-204. Particularly, the analysis reveals Cleaved Caspase-3 positive cells in each sample. (b) The graph indicates the percentage of Cleaved Caspase-3 positive cells in LNA-CT (black) and LNA-204 (red) sample. N=7 per each sample. **p<0.01.

Finally, to make sure that LNA worked *in vivo,* we estimated the levels of the endogenous miR-204 using specific primers for the mouse species. As indicated by qRT-PCR analysis, following LNA-204 transfection, the expression level of miRNA significantly decreases (Figure 37).

We concluded that LNA-204 works *in vivo* as well as *in vitro* and the observed biological effects (increased apoptosis and decreased proliferation) are dependent on miR-204 inhibition.

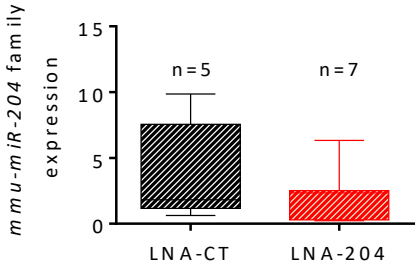

Figure 37. LNA-204 inhibits the endogenous miR-204 *in vivo* as *in vitro*.
Mmu miR-204 expression level is measured by qRT-PCR analysis in mouse tumor samples after the injection of LNA-CT (black) or LNA-204 (red). After the transfection of LNA-204 miR-204 level decreases compared to the control. N=7 per each sample.

An aspect to be examined further is the onset of toxic effects associated with the transfection of LNA-204 and, for this purpose, we monitored the weight of the animals in which we

performed the injections. As shown in the graph (Figure 38), there were no relevant changes in the weight of mice during the period of treatment. The absence of weight loss indicates that LNA-204 injections do not cause overall toxicity.

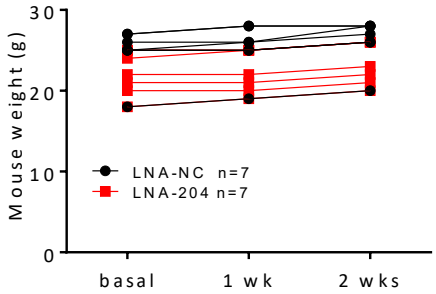

Figure 38. LNA-204 doesn't cause overall toxicity.
The curve represents the trend of mice weight during the weeks of treatment with LNA-CT (black) or LNA-204 (red). LNA-204 injections do no cause weight loss ascribable to toxicity.

4.4. The molecular mechanism through which LNA-204 induces apoptotic cell death

After demonstrating the pro-apoptotic action of LNA-204 both *in vitro* and *in vivo* model systems, I explored the molecular mechanisms that trigger the apoptotic process. I also attempted the identification of miR-204 target(s) that get(s) derepressed by LNA-204 and induce apoptosis.

4.4.1. LNA-204 induces p53 protein stabilization and cytoplasmatic localization

Since p53, a known tumor suppressor, as nuclear transcription factor regulates the expression of numerous genes involved in apoptosis, I estimated its expression level by means of Western blot analysis. I transfected 60nM LNA-204-MM or LNA-204 in A375, which express wild-type p53, and SkMel-28 cells, which express mutant p53, performing a time course, and I observed the early induction of p53 protein (6h post-transfection of LNA-204) in A375 cells, while in SkMel-28 cells the increase appears at 24h (Figure 39).

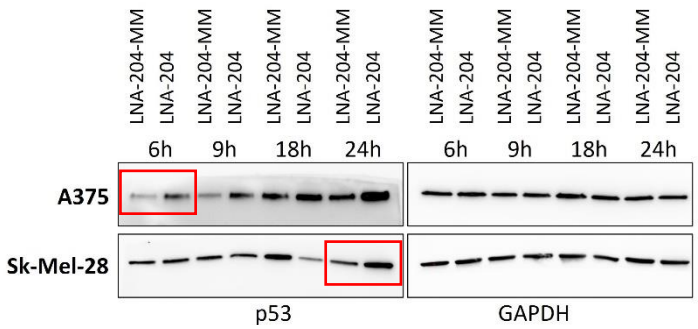

Figure 39. LNA-204 induces the increment in p53 protein.
WB analysis shows p53 protein expression level at 6h, 9h, 18h and 24h after the transfection of 60 nM LNA-204-MM or LNA-204 in A375 (wild-type p53) and SkMel-28 (mutated p53). In A375 the increment in p53 levels is detected at 6h, while in SkMel-28 at 24h. A representative of 3 independent experiments is reported.

Then, I confirmed the increment in p53 levels at 6h after the inhibition of miR-204 in several melanoma cell lines, as shown in Figure 40.

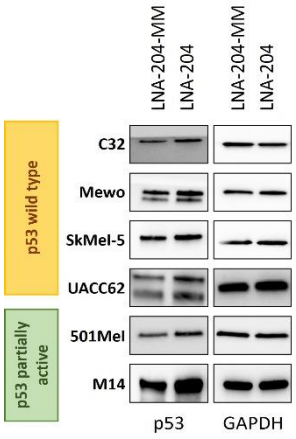

Figure 40. The induction of p53 protein expression on several melanoma cell lines.
WB analysis shows p53 protein levels at 6h from the transfection of 60 nM LNA-204-MM or LNA-204 in C32, SkMel-5, UACC62 (wild-type p53) and 501Mel, Mewo, M14 (mutated p53). LNA-204 induces p53 expression on all analyzed cell lines. A representative of 2 independent experiments is reported.

The early induction of p53 represents a possible explanation, maybe not the only one, for the activation of caspases at 18h after the transfection of LNA-204, as shown in Figure 12, and the apoptosis observed at 24h, as shown in Figure 24. This hypothesis is supported by the results obtained in NCI-H358 (lung cancer) and SkMel-28 cells. In p53 null NCI-H358 cells (Figure 41a) the apoptotic effect of LNA-204 is very faint (Figure 41b), while in SkMel-28 the increase in p53 levels at 24h rather than 6h post transfection is consistent with the fact that I saw a mild, not significant, increase in the percentage of cells in sub-G1 phase of cell cycle (Figure 42a) and of apoptotic cells (Figure 42b), which in addition occurred at 48h instead of 24h as for the other cell lines discussed.

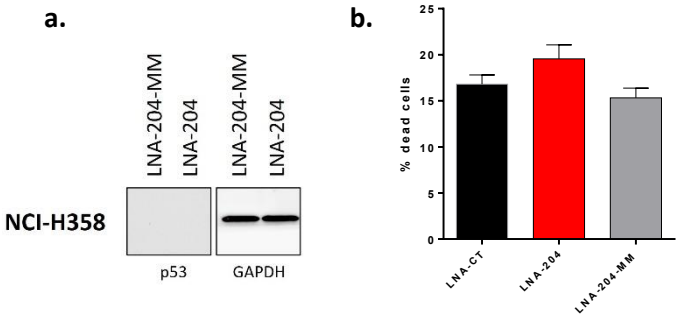

Figure 41. Quantification of apoptosis induced by LNA-204 in p53-/- NCI-H358 cells.
(a)The Western Blot analysis confirms the absence of p53 protein in NCI-H358 cells. (b) The graph shows the percentage of dead cells at 48h after the transfection of LNA-NC (black), LNA-204 (red) or LNA-211 (blue) in NCI-H358 cells. LNA-204 induces a mild increase in apoptosis at 24h from the transfection. The mean ± SEM of 2 independent experiments is reported.

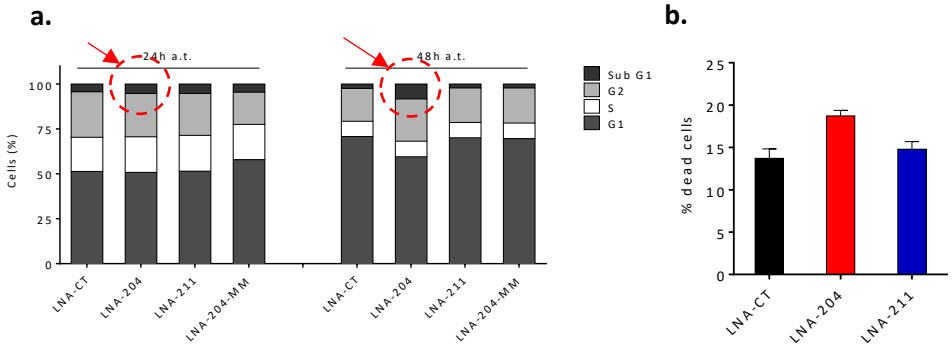

Figure 42. The effect of LNA-204 in SkMel-28.
(a) The bar graph represents cell cycle analysis performed at 24h and 48h post transfection of the indicated LNA-CT, LNA-204-MM, LNA-204 or LNA-211 in SkMel-8. The percentage of cells in sub-G1 is highlighted in red. As shown, LNA-204 induces a mild increase of cells in sub-G1 phase of cell cycle at 48h from the transfection. LNA-211 has not effect. The results of 1 experiment are reported. (b) The figure shows the percentage of dead cells at 48h after the transfection of LNA-NC (black), LNA-204 (red) or LNA-211 (blue) in SkMel-28. LNA-204 induces a mild increase in apoptosis at 48h from the transfection instead of 24h as reported in Figure 24. The mean ± SEM of 3 independent experiments is reported.

Definitely, the data revealed a correlation between the apoptosis, induced by LNA-204, and the activation of p53-signaling. Next, to better comprehend the mechanism of p53 induction, I transfected A375 cells with 60nM LNA-204-MM or LNA-204 and at 5h after the transfection I treated them with cycloheximide, an inhibitor of protein synthesis, for 1h. The use of cycloheximide evidenced that the change in p53 expression is not associated with increased transcription (Figure 43a), but it is due to a post-translational modification that leads to protein stabilization (Figure 43b and 43c).

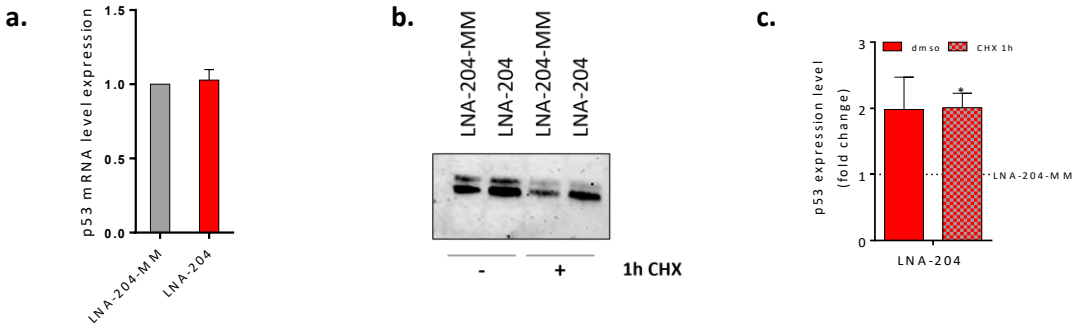

Figure 43. LNA-204 induces p53 protein stabilization.
(a) Quantification of p53 mRNA level expression by Real Time PCR in A375 cells at 6h from the transfection of LNA-204-MM (grey) or LNA-204 (red). (b) Western blot analysis shows p53 levels after 1h of treatment with cycloheximide in A375 cells transfected with LNA-204-MM or LNA-204 5h earlier. A representative of 3 experiments is reported. (c) Fold change increase in p53 expression levels. The mean ± SEM of 3 independent experiments (mentioned in b) is reported. *p<0.05.

In addition, in order to localize the stabilized p53 protein I performed the nucleus-cytoplasm fractionation in A375 cells, at 6h after the transfection of LNA-204-MM or LNA-204. As indicated by Western blot analysis in Figure 44, I detected a statistically significative

increment of p53 expression in the cytoplasm after the transfection of LNA-204 compared to LNA-204-MM. Moreover, I confirmed the data by means of immunofluorescence experiment (Figure 45). Based on these results, I propose that stabilized p53 plays its peculiar role in the investigated mechanism, possibly through both the cytoplasmatic and nuclear fraction.

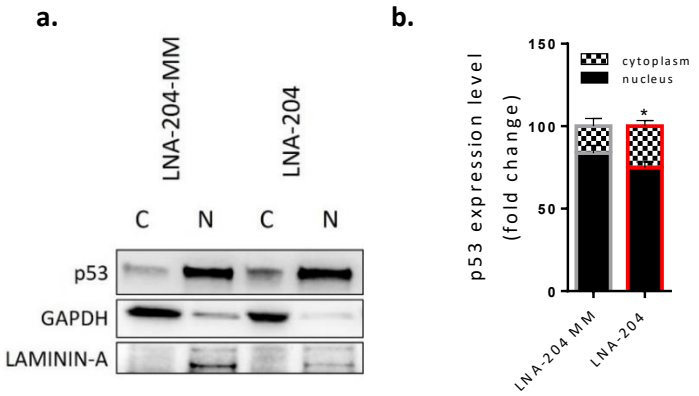

Figure 44. **p53 protein levels increase in cytoplasm after the transfection of LNA-204.**
(a) Western blot analysis shows nuclear and cytoplasmic p53 protein expression level at 6h after the transfection of 60 nM of LNA-204-MM or LNA-204. A representative of 4 experiments is reported. (b) Fold change increase in nuclear p53 expression level is measured. The mean ± SEM of 4 independent experiments (mentioned in a) is plotted. *p<0.05.

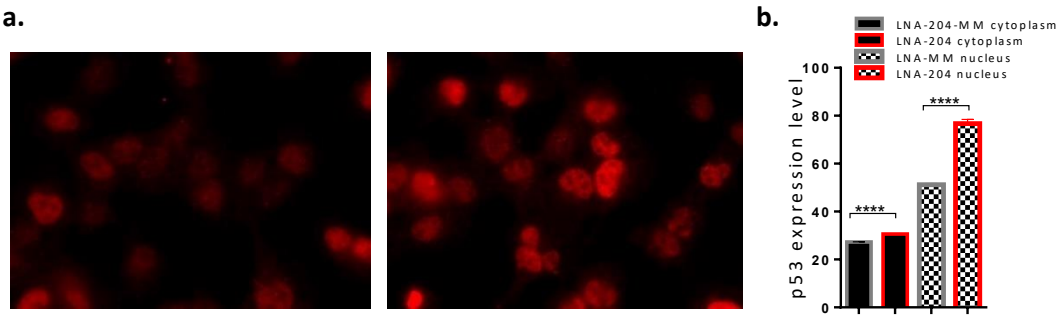

Figure 45. Immunofluorescence confirms the increase in nuclear p53 protein level at 6h from LNA-204 transfection.
(a) The figure contains illustrative pictures of the immunofluorescence performed in A375 cells at 6h after the transfection of 60nM of LNA-204-MM or LNA-204. p53 protein is represented by red fluorescence: nuclear and cytoplasmatic signal is stronger after the transfection of LNA-204 compared to the negative control. (b) Quantification of p53 expression level in nucleus and cytoplasm relative to the pictures in a. The mean ± SEM of 1 experiment is reported. ****p<0.0001.

4.4.2. The identification of a specific and direct miR-204 target which mediates the apoptosis

Once understood the involvement of p53 in the phenomenon, I proceeded with the identification of a specific miR-204 target, which, derepressed when the miRNA is inhibited, mediates the apoptosis. To achieve this aim, in light of the fact that p53 is induced as early as 6h after LNA-204 transfection, I performed an RNA-sequencing at 6h after the transfection of LNA-204-MM or LNA-204 in A375 and 501Mel cells. From the analysis of sequencing data,

I acquired a list of up-regulated (red, 3156) and down-regulated (blue, 2904) differentially expressed mRNAs in LNA-204 samples of both cell lines. Since when miR-204 is inhibited by LNA-204 the target gene is derepressed and it should be up-regulated, I focused the attention on up-regulated ones in common between A375 and 501Mel. Subsequently, to be more stringent, I considered the genes with a fold change greater than or equal to 1.5 in both lines. Applying this criterion, I obtained a short list of 21 genes: for each of them I studied the known role in literature and, based on this, I divided them into 4 classes (Figure 46). However, I delved into the characterization of genes belonging to the first two classes (green and yellow) and excluded those implicated in biological processes not linked to the apoptotic phenotype (grey), as well as those directly related to apoptosis (orange), as I assumed that the target to be identified is connected to earlier intracellular events that ultimately lead to apoptosis. I summarized the procedure in Figure 46.

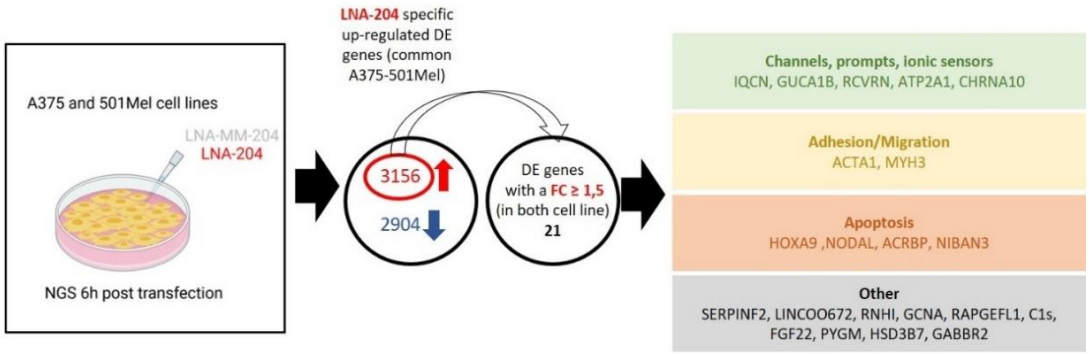

Figure 46. RNA-sequencing: from cells to analysis.
The figure summarizes the steps from cells transfection to the data analysis. The RNA-sequencing is performed on A375 and 501Mel cells at 6h from the transfection of LNA-204-MM or LNA-204. The upregulated differentially expressed mRNAs with a FC≥1,5 in both cell lines (21) is divided into 4 classes in according to the literature. The mRNAs belong to the first (green) and the second (yellow) class are selected for further investigation.

4.4.2.1. Channels, prompts, ionic sensors

The first class includes genes coding for channels, prompts and ionic sensors. I reported the list in Figure 47.

Figure 47. The class of channels, prompts and ionic sensors.
List of genes belonging to the first class and coding for channels, prompts and ionic sensors.

In order to reduce as much as possible the number of candidate genes among which to find one or more miR-204 targets, I estimated the expression levels of mRNAs listed in Figure 47 by qRT-PCR, by overexpressing (204-mimic) or by inhibiting (LNA-204) endogenous miR-204 in A375 cells. In both experimental conditions I evaluated AP1S2 mRNA levels as a positive control because in *Vitiello et al.* [20] it was identified as miR-204 direct target when the miRNA is overexpressed. As shown in the bar graph in Figure 48, when the miRNA is overexpressed by using 204-mimic, AP1S2 expression is indeed significantly decreased compared to si-CT. On the contrary, when miR-204 is inhibited by LNA-204, its expression does not change. I selected as final genes to characterize those which show increased expression following miRNA inhibition and a decreased or unaltered expression when the miRNA is overexpressed.

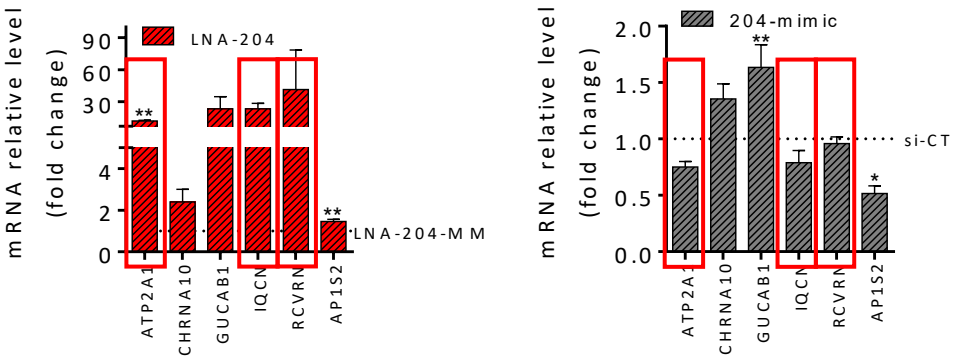

Figure 48. Expression level of ATP2A1, CHRNA10, GUCAB1, IQCN and RCVRN.
The graph shows a fold increase in the mRNA levels of the indicated genes at 6h after the transfection of LNA-204-MM or LNA-204 (left) and at 24h after the transfection of si-CT or 204-mimic (right). AP1S2 is used as a control. According to the trend the highlighted genes are selected for the validation. The mean ± SEM of 3 independent experiments is reported. *p<0.05; **p<0.01.

The selected genes are ATP2A1, IQCN and RCVRN. Interestingly, the case of AP1S2 on one side and ATP2A1, IQCN and RCVRN on the other indicate that the double function of miR-204 (anti migration/invasion when overexpressed and proapoptotic when inhibited) is associated with the modulation of distinct gene sets. ATP2A1, IQCN and RCVRN were characterized further. I found that they are induced as early as 4h after the transfection of LNA-204, but not of LNA-211 in a wide spectrum of melanoma cell lines (Figure 49). These results indicated that their up-regulation is specifically correlated with the inhibition of miR-204, but not of miR-211.

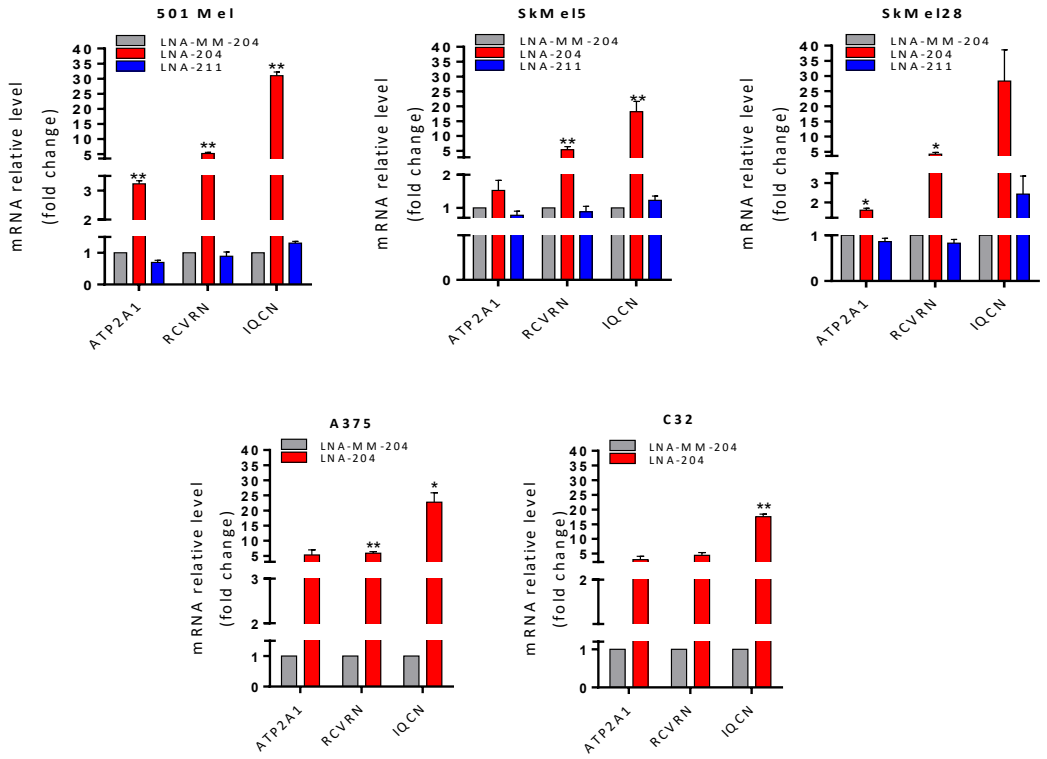

Figure 49. mRNA expression level of ATP2A1, IQCN and RCVRN on several melanoma cell lines.
The graph shows the fold increase in the mRNA levels of the indicated genes at 4h after the transfection of LNA-204-MM (grey), LNA-204 (red) or LNA-211 (blue) in A375, C32, SkMel-5, 501Mel and SkMel-28. The increase is specifically induced by LNA-204, but not LNA-211. The mean ± SEM of 2 independent experiments is reported. *p<0.05; **p<0.01.

A relevant feature in common among the 3 genes is their involvement in calcium signaling. ATP2A1 (SERCA1) is a pump located on the membrane of the endoplasmic reticulum (ER) and transports calcium from the cytosol to the ER. RCVRN codifies for a protein (Recoverin) that works as a calcium-sensor. IQCN contains the IQ motif, a calmodulin binding sequence. Therefore, I theorized that the apoptosis induced by LNA-204 was calcium dependent. In order to demonstrate it, I used a lentiviral plasmid containing a calcium sensor, the GcAMP6s. It derives from the fusion of GFP (green fluorescent protein), calmodulin and M13 peptide [31]. If the intracellular calcium concentration increases, the ion binds to calmodulin. The interaction causes a conformational change in GFP structure with the emission of green fluorescence. Once obtained the lentivirus, I stably infected A375 cells and I created the stable cell line that constitutively express the construct (A375-GcAMP6s).

Since GcAMP6s is a calcium sensor commonly used in neurons, to make sure it worked in A375-GcAMP6s, I performed a preliminary experiment by treating the cells with thapsigargin. The drug is a SERCA1 inhibitor and causes an intracellular increase in calcium levels. Indeed,

as evidenced in Figure 50, after 5 minutes of treatment, I observed a profound increment in fluorescence.

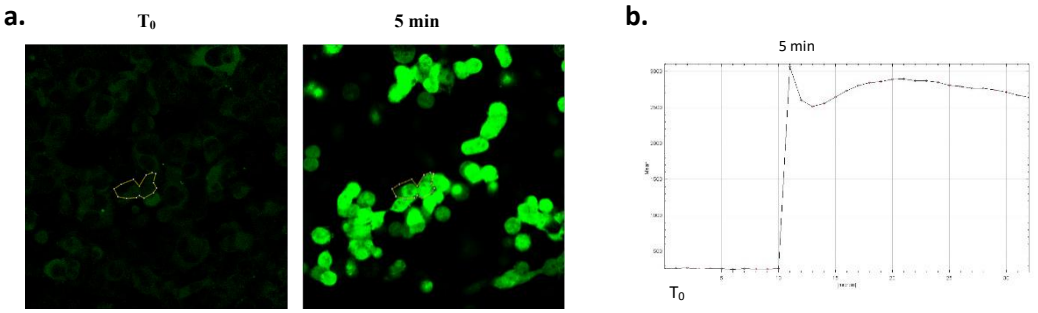

Figure 50. A375-GcAMP6s responsiveness to the treatment with thapsigargin.
a) Representative pictures of A375-GcAMP6s treated with thapsigargin. (Left) Cell fluorescence at T=0; (right) increased fluorescence after 5 minutes of treatment with 3µM thapsigargin. (b) Curve of fluorescence along 15 minutes from the start of treatment. The values of 1 experiment are plotted in the curve.

Validated the sensitivity of the construct to calcium level variations in melanoma cells, I transfected 60nM LNA-CT or LNA-204 in A375-GcAMP6s and performed a Time-Lapse experiment at the confocal microscope (Zaiss, 20X at air lens) to register changes in calcium concentration into the cells. I started monitoring the fluorescence approximately 2h after the transfection of LNA-204: as shown in Figure 51, 124 minutes later (4h post transfection) the signal increases in LNA-204 sample compared to the negative control and maintains the trend until the end of the experiment. Based on results of the first experiment, it seems that miR-204 inhibition induces a change in calcium level, but it's necessary to repeat it and confirm the data.

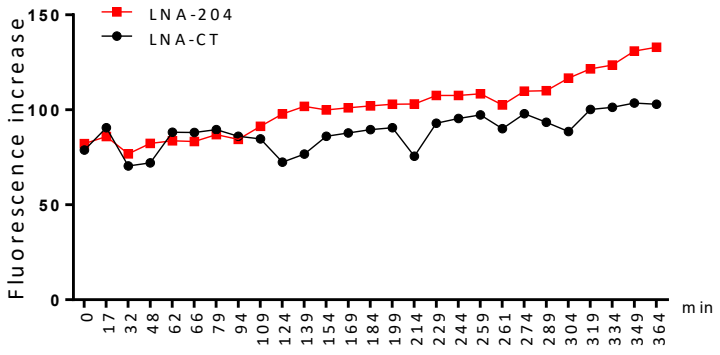

Figure 51. Measurement of intracellular calcium concentration through GcAMP6s fluorescence.
The curve represents the fluorescence of A375-GcAMP6s after the transfection of LNA-CT (black) or LNA-204 (red) from 0 min (about 2h post transfection) to 364 min (about 8h post transfection). At 124 minutes the signal increases in LNA-204 sample compared to the negative control. The results of 1 experiment are plotted.

Meantime, I proceeded with the characterization of each gene. As explained in Material and Methods, I have already cloned RCVRN and IQCN coding sequence in pCW, an inducible vector (Figure 52).

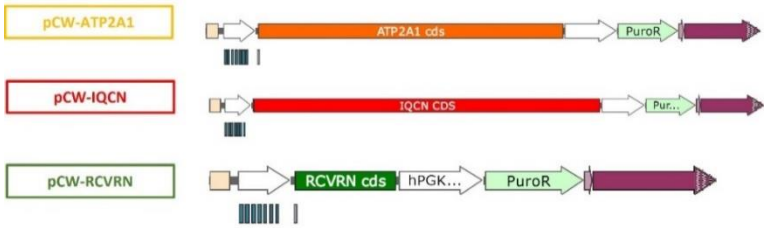

Figure 52. Map of inducible pCW vector containing ATP2A1, IQCN and RCVRN coding sequence.
The vectors are used to stably overexpress ATP2A1, IQCN and RCVRN protein in A375 cells.

After cloning, I produced the corresponding lentivirus and, lastly, I created a stable cell line in A375 cells, overexpressing each of them. Once expanded the cells, I quantified the expression of gene by qRT-PCR in order to validate gene overexpression (Figure 53).

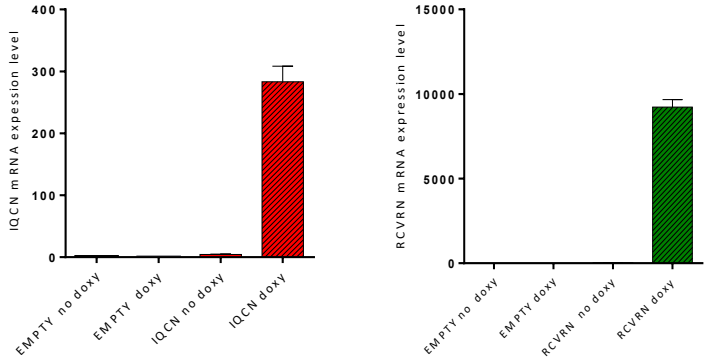

Figure 53. Validation of stable IQCN and RCVRN overexpression in A375 cells by means qRT-PCR.
The graph bar shows a fold increase in IQCN and RCVRN mRNA expression level in stable A375 cells at 24h from the induction with doxycycline 2µg/mL.

Then, I transfected A375-IQCN or A375-RCVRN with 60nM LNAs. If the gene is a target of miR-204 and, in particular, the mediator of the apoptosis, overexpressing it I should observe an increment in the percentage of apoptotic cells compared to the cells only transfected with LNA-204. Unfortunately, I didn't observe the expected increase in apoptosis.

Regarding ATP2A1, the cloning in pCW is ongoing. In the literature, many works have revealed the existence of a mechanism in which apoptosis is induced by the interaction between ATP2A1 (SERCA1) and p53 in the endoplasmic reticulum. Thus, I aimed to investigate the colocalization of the two proteins, in order to understand if it can explain the appearance of apoptosis after LNA-204 transfection. To overexpress ATP2A1, for now I used

the vector pCMV6 containing human ATP2A1 ORF (Myc-DDK-tagged) (OriGene, #RC216526). The map of the plasmid is illustrated in Figure 54. As a negative control, I utilized pCMV empty. I performed the experiment in A375-SEC61B, a cell line stably overexpressing SEC61B (green), which is a ER membrane marker.

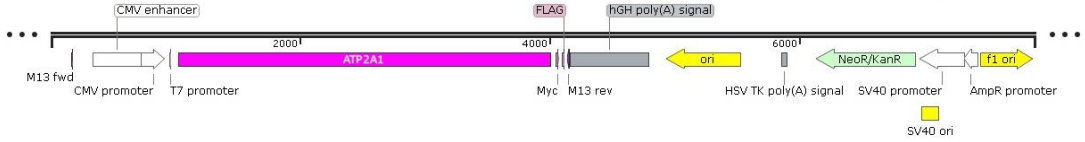

Figure 54. Map of pCMV6-ATP2A1 (Myc-DDK-tagged) vector (OriGene).
The vector is used to transiently overexpress ATP2A1 in A375 cells.

I transfected pCMV empty and pCMV6-ATP2A1 (Myc-DDK-tagged) in A375-Sec61B. After 48h from the transfection (the time necessary for the exogenous protein to express itself), I performed an immunofluorescence and used a primary antibody against Myc tag (red) to mark ATP2A1 protein and to visualize its localisation into the cells. As expected, in the negative control it is visible only the green signal because Myc antibody is not able to bind the endogenous protein, instead in cells overexpressing ATP2A1 the signal of red fluorescence is very intense and it merges with green signal. The presence of red signal proved the expression of the exogenous protein, while the overlapping between green and red around the nucleus confirms the localization of ATP2A1 in ER like SEC61B (Figure 55).

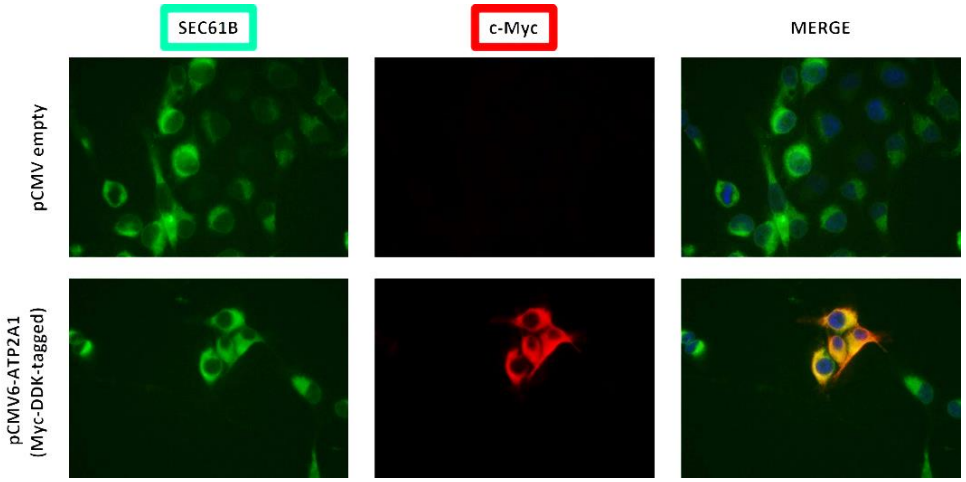

Figure 55. Exogenously overexpressed ATP2A1 colocalizes with SEC61B in ER membrane.
Illustrative pictures of immunofluorescence at 48h after the transfection of pCMV6-ATP2A1 (Myc-DDK-tagged) in A375-SEC61B. The fluorescence of SEC61B (green) and ATP2A1 (red) are detected. SEC61B and ATP2A1 colocalization in ER membrane is represented by merged signal (yellow).

Once demonstrated the functioning of vector, I will transfect it in A375. After 48h, I will re-transfect the cells with 60nM LNA-NC or LNA-204. 6h later I will fractionate ER and

expect to see an increase in p53. I also expect that p53 and ATP2A1 colocalize at ER. Finally, I expect that ATP2A1 overexpression and LNA-204 cooperate in apoptosis induction.

4.4.2.2. Adhesion/migration

The genes included in the second class belong to the adhesion/migration process (Figure 56).

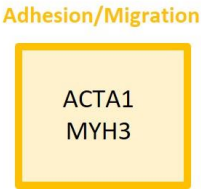

Figure 56. The class of adhesion/migration genes.
List of mRNAs belonging to the second class and coding for proteins involved in adhesion/migration processes.

I'm currently characterizing each one. However, I already performed the adhesion assay and I found that, 9h after the transfection of 60nM LNA-204, a strong reduction in the number of adherent cells is observed in comparison to LNA-204-MM. I initially observed this decrease in A375 cells and, then, confirmed it in 501Mel, UACC62 and COLO800 cells (Figure 57).

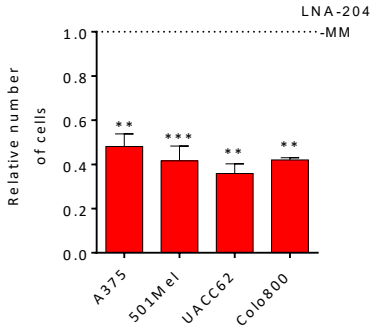

Figure 57. LNA-204 causes a decrease in cell adhesion in melanoma cell lines.
The bar graph shows the number of adherent cells at 9h after the transfection of LNA-204-MM or LNA-204 and 30 minutes from seeding in A375, 501Mel, UACC62 and Colo800. A fold decrease is induced by LNA-204. **p<0.01; ***p<0.001.

4.4.3. Conclusions so far

In Figure 58 a conclusive cartoon to summarize my findings (to date) for each time point after LNA-204 transfection. At 4h from the transfection (yellow box), LNA-204, but not LNA-211, induces the upregulation of ATP2A1, IQCN and RCVRN. Up to now, I am unable to provide an explanation of their expression increase. At 6h from the transfection (blue box) p53 is

stabilized and its levels increase both in the nucleus and in the cytoplasm, while at 9h loss of adhesion (red box) is observed. At 18h from the transfection of LNA-204, there is the activation of both the intrinsic and the extrinsic apoptotic pathways (green box), which precedes the increased apoptosis (violet box) at 24h. The apoptosis is the consequence of the early intracellular events (genes upregulation, p53 induction and loss of adhesion). The experimental data don't allow me to assert whether the three events occur independently or if they are the cause of each other. It's also possible that the genes upregulation, the induction of p53 and the loss of adhesion occur independently, but are triggered by the same cause. I hypothesize that the cause could be a very early alteration in calcium homeostasis, since it's very well known the relation between the calcium signaling and the upregulated genes role, the proapoptotic activity of p53 and cell adhesion.

In conclusion, further experimental work is necessary to establish the molecular mechanism through which LNA-204 induces such a strong and specific apoptosis in melanoma cells.

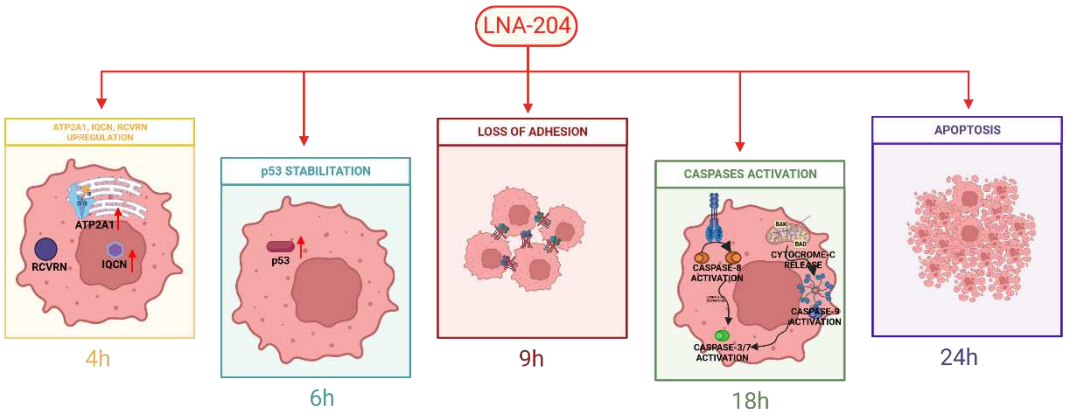

Figure 58. Cartoon summarizing the findings for each time point after LNA-204 transfection.
In the pictures the findings for each time point after LNA-204 transfection is represented in a coloured box: in yellow (4h) the upregulation of ATP2A1, IQCN and RCVRN; in blue (6h) the induction of p53 pathway; in red (9h) the loss of adhesion; in green (18h) the activation of caspases; in violet (24h) the increased apoptosis.

5. Discussion

As proven by numerous studies published in literature, miR-204 plays a tumor-suppressive role by regulating various processes, such as proliferation, apoptosis, invasion/migration, metastasis, autophagy, EMT, anticancer drug sensitivity and immune microenvironment, in many types of solid tumors, including melanoma [23][21][32]. However, in some cancer settings, particularly as seen in prostate cancer [33] and breast cancer [34][35][36][37], it performs a dual role and acts as both a tumor suppressor and an oncogenic miRNA.

In according with its tumor inhibitory activity, miR-204 is down-regulated in human cancers compared to normal tissue [38][39][40]. As reported in [24][41], also in melanoma samples its expression is lower than in benign nevi, and, precisely, in metastatic melanomas is reduced compared to primary tumors. This has clinical relevance, as it has been seen in patients that lower miRNA expression is associated with worse prognosis. Since miR-204 interferes with tumor progression, restoring its expression could be a strategy to enhance its tumor-suppressive effects. In fact, it has been demonstrated that, in melanoma cells, miRNA overexpression leads to a reduction in cell migration/invasion capacity [20][42], cell proliferation and colony-forming ability [42].

In this work, I presented the results obtained with miR-204 inhibition using LNA-204, a specific inhibitor. In light of the data shown in the papers mentioned so far, I expected to observe oncogenic effects i.e. an increase in cell migration/invasion, proliferation and number of colonies. Indeed, contrary to expectations, following miRNA inhibition, a decrease in proliferation and a dose-dependent increase in apoptosis was detected. Based on this, I supposed that, in melanoma cells, miR-204 role depends on expression level and I hypothesized that it has a *lineage survival* function, so its presence is essential for cells to remain alive. The hypothesis is in contrasts with the tumor suppressive action discussed in the majority of works, but is supported by the fact that in melanoma samples TRPM3/miR-204 locus is not lost or inactivated like normally occurs for other known tumor suppressors [43]. The antiproliferative and proapoptotic consequences of LNA-204, initially investigated in cultured cells, were consolidated in *in vivo* model systems (zebrafish, mouse), where miR-204 inhibitor suppresses tumor growth reducing proliferation and promoting apoptosis. In clinic, the most common rout of administration for the anticancer drugs is the systemic route. However, in our case, the LNA-204 exhibits its proapoptotic and antiproliferative effects not only on melanoma cells, but also on melanocytes. Thus, to overcome the problem in *in vivo* models, the LNA-204 was administrated through intratumoral injections. An alternative

approach to the systemic rout that we are exploring in our lab consists in conjugating LNA-204 to the peptidoglycan of *attenuated Listeria monocytogenes*. The use of the *Listeria* as a carrier of drug brings numerous advantages, including the selective tropism for tumor cells, allowing to increase the therapeutic effect and at the same time to minimize the collateral effects related to systemic administration.

An important aspect that I considered is the comparison between miR-204 and miR-211 inhibition by using respectively LNA-204 and LNA-211, since the two miRNAs, belonging to the same family, differ in sequence by only two bases. Once the specificity of each LNA for its intended miRNA target was validated, I demonstrated, in both *in vitro* and *in vivo* experiments, that the biological effects observed are specifically due to the de-repression of one or more mRNAs following the suppression of the endogenous miR-204, but not of miR-211. As explained in [44], it's generally assumed that microRNAs included in the same family carry out redundant functions and, for this reason, the target genes are predicted for the miRNA family instead of the single miRNA. Contrary to this assumption, the results collected here suggest that, even though they are sisters miRNAs, miR-204 and miR-211 bind to distinct targets and, consequently, don't produce equal biological effects. The presence of two dissimilar bases, at 3'end, between the two sequences determines a difference in genes specificity. Indeed, there are other cases of miRNAs of the same family (in particular the examined cases concern let-7, miR-48, miR-84 and miR-241), with identical seed sequence, similar sequence at seed-distal 5' and mismatched sequence at seed-distal 3', that regulate the expression of different pools of mRNAs. The interesting discovery is that a perfect and extended miRNA-target pairing at the seed-distal 3' determines specificities in target silencing by a single miRNA of the family even if the seed region match is perfect [45][46]. This finding is in line with the architecture of my miRNAs, especially with the position of the two discriminating bases and, as future perspective, it will be interesting to experimentally validate it. In addition, it has already been demonstrated that, when they are overexpressed, miR-204 and miR-211, repressing different genes, are mediator of independent biological outcomes and this diversification depends on the cellular context in which they are expressed [20].

Regarding the proapoptotic activity of LNA-204, the increase in caspase-8, caspase-9 and caspase-3/7 activity indicates that there is not a prevalent pathway, but both intrinsic and extrinsic pathways are activated. A possible explanation of these data is the crosstalk among the two signaling. The key mediator is represented by BID protein. In presence of apoptotic stimuli, cell death receptor (extrinsic way) triggers the activation of caspase-8 which in turn cleaves BID protein. The cleaved protein, tBID, translocates to mitochondria where it interacts

with Bax and Bak promoting the permeabilization of mitochondrial membrane with subsequent release of cytochrome-c and the activation of the extrinsic signaling that leads to the activation of caspase-9 [47][48][49][50]. As previously mentioned, contrary to the *lineage survival* function that I hypothesized on the basis of the results obtained by inhibiting it with LNA-204, in most of the literature the tumor suppressive activity of miR-204 is demonstrated. In particular, it induces apoptosis by repressing the expression of BCL-2 (antiapoptotic protein) involved in the intrinsic pathway [51]. In order to reconcile these opposite behaviours, I suppose that, in suffering conditions due to the effects of LNA-204, cells communicate with each other by sending signals that determine the activation of Death Receptors (extrinsic pathway) and then, through the activity of BID, the activation of intrinsic pathway. Furthermore, it's possible that caspase 3/7, once cleaved by caspase-9, activates caspase-8, to amplify the cell death signal, regardless of Death Receptor dimerization [52]. Ultimately, in order to better define the contribution of each pathway, it would be useful to measure caspases activity following the transfection of LNA-204 into cells in which the Death Receptor is inhibited (for example by overexpressing the c-FLIP protein) or caspase-8 is inhibited (Z-IETD-FMK).

Next, after having consolidated the anti-cancer effects of miR-204 inhibition in cell cultures and animal models, I explored the molecular mechanisms through which the apoptosis occurs, and I established that a correlation exists between LNA-204-induced apoptotic cell death and the induction of p53 signaling. I came to this conclusion after analysing a large number of melanoma cell lines that I selected based on the mutational status of p53 reported in already published articles and confirmed in my cells through sequencing. I observed p53 induction at 6h from the transfection, followed by a strong increment in the percentage of apoptotic cells at 24h, in A375, C32, Mewo, SkMel-5 and UACC62 that express a wild-type protein [53][54][55][56]. Similar results have been obtained also in M14 and 501Mel in which p53 is mutated. Particularly, M14 cells carry the mutation p.G266E (in heterozygosity) identified in [55], while in 501Mel I found p.C275W (in homozygosity) in agreement with [57]). On the other hand, SkMel-28 show the mutation p.L145R [53][55][58], but in this case I measured the increment in p53 expression at 24h after the transfection of LNA-204, rather than at 6h, and a mild, not significant, increase in apoptosis at 48h, not at 24h like in other mutated or wt cell lines. The proapoptotic effect of LNA-204 is very faint also in NCI-H358 cells, a lung cancer cell line in which p53 is not expressed.

As written on OncoKB^{TM} database, all p53 mutations, mentioned previously, belong to the DNA binding domain and affect p53 transcriptional transactivation. However, p.G266E (M14)

and p.C275W (501Mel) are classified as "*likely oncogenic*" and cause the expression of a partially active p53. Instead, p.L145R (SkMel-28) is categorized as *"oncogenic"* mutation: it has been found in melanoma and leads to loss of function. As a result, the protein is not functional [58][59], mimicking the complete absence of p53 that characterize NCI-H358 cells. Thus, the impact of these genetic alterations on p53 activity as tumor suppressor, in particular its proapoptotic role, demonstrate the existence of a correlation between apoptosis and p53 induction. Moreover, the preliminary data in A375 showing the early (6h after-transfection) increment in p53 protein levels in cycloheximide treated cells implies that the change in its expression is not attributable to transcriptional regulation, but to various types of post-translational modifications that cause its stabilization and, hence, the elongation of its half-life [60][61][62][63]. However, to be able to state that LNA-204 induced cell death depends on p53 signaling is necessary to observe a rescue by using a specific chemical inhibitor of the protein.

Other relevant aim of the work was the identification of miR-204 target(s) by means an RNA-Sequencing performed at 6h from the transfection of LNA-204. ATP2A1, IQCN and RCVRN are selected as candidate genes of the first class *(channels, prompts, ionic sensors)*. I'm analysing the role of each gene and to date, it remains to be established whether they are direct miR-204 targets and/or their transcription is under p53 control. However, the interesting aspect to explore further is the involvement of each one in calcium signaling [64][65][66]: preliminary data show an increment in calcium levels 4h after the inhibition of miR-204 and this change in intracellular calcium concentration occurs at the same time point as the upregulation of ATP2A1, IQCN and RCVRN. So, it remains to be established whether these two events are linked to each other and whether one is the cause of the other.

Among the 3 genes, I focus the attention on ATP2A1 because I found many papers in which it has been studied in relation with p53. It's known that, in response to stressful stimuli, p53 is activated and, in the nucleus, as a transcription factor, it regulates the expression of genes involved in apoptosis and other processes. In addition, the cytoplasmatic protein interacts, by means of the DNA-binding domain, with Bcl-2 (anti-apoptotic protein) and Bak (pro-apoptotic protein) and induces the permeabilization of mitochondrial membrane with the release of cytochrome-c [67][68]. Recently, a new pro-apoptotic role of cytoplasmatic p53 was highlighted: a role Ca^{2+}-dependent, but transcription and DNA-binding domain-independent. ATP2A1 represents a target of p53 transcriptional activity because its promoter contains a binding site for the transcription factor (GeneCard). It is also implicated in a novel mechanism through which p53 act as tumor suppressor and exhibits its ability to promote apoptosis.

The evidence suggests that, following apoptotic stimuli, p53 activates and accumulates in MAMs (mitochondrial-associated-membranes) and ER where it binds to SERCA1 (ATP2A1) pump through C-terminal domain. The interaction triggers a change in oxidative state of the pump and then the transfer of calcium from ER to mitochondria. But, mitochondrial calcium influx is toxic. Consequently, the permeabilization of the membrane with the release of cytochrome-c and the activation of the intrinsic apoptosis pathway occur [69]. Given the strong correlation p53-apoptosis, the increment in p53 levels in the cytoplasm and ATP2A1 upregulation after 6h from LNA-204 transfection, the process described above could explain the different trend of apoptosis which distinguishes A375, C32, Skmel-5, UACC62, M14, 501Mel, Mewo from SkMel-28 and NCI-H358: besides cell lines carrying wt p53, in M14 and 501Mel, p53, being partially active and carrying mutation outside C-terminal domain, can still interact with SERCA1 and induce cell death. Conversely in SkMel-28, the complete loss of function affects this capacity.

I'm investigating also a second class of genes derived from the analysis of RNA-seq data and involved in adhesion/migration. The reduction in cell adhesion, observed 9h after the transfection of LNA-204, may be an additional consequence to the imbalance in calcium levels since adhesion molecules are calcium-dependent. Since melanoma cells are adherent cells, I propose that the loss of the ability to adhere represents a negative stimulus that triggers apoptotic cell death as demonstrated in [70].

Meanwhile, I'm attempting to identify the initial trigger trough which LNA-204 can induce apoptosis. TRPM3 is miR-204 host gene and a direct target: a regulatory loop exists between miR-204 and TRPM3, particularly, the inhibition of miR-204 causes the accumulation of TRPM3 protein [22]. The increase in protein level supports the absence of TRPM3 in upregulated mRNAs list after the transfection of LNA-204. In addition, TRPM3 codifies for a calcium channel. Its rapid accumulation at protein level would be consistent with the observed increment in calcium concentration and might represent the initial trigger of the process.

In conclusion, the inhibition of miR-204, by using LNA-204, could have a clinical impact and be exploited to develop an alternative therapeutic strategy for the treatment of melanoma, since it induces massive apoptosis. To explain the apoptotic phenotype associated with miR-204 inhibition, we are exploring three different aspects: the SERCA1-p53 interaction, the loss of adhesion and the involvement of the calcium pathway. However, the data obtained to date do not allow us to assert with certainty the mechanism through which apoptosis occurs, whether one aspect is consequential to the other or whether these different

mechanisms are activated simultaneously as distinct effects of LNA transfection. Additionally, it's necessary to repeat many experiments in other cell lines in order to consolidate the obtained results and to be sure that the mechanism is not cell line-dependent.

In the last years, we have analysed a large number of possible target genes, using different strategies. Initially, considering the increase in apoptosis at 24h from LNA-204 transfection, we performed an array at the same time point focusing on the proapoptotic genes. However, we could not identify direct targets of miR-204. Only subsequently, having detected the induction of p53 much earlier, we performed the RNA-sequencing at 6h post transfection and we are analysing the genes involved in calcium signaling and adhesion/migration, early events that could lead to cell death. Based on our experience and in light of the fact that each miRNA can have a lot of targets, we hypothesize that LNA-204-induced apoptosis is a complex phenomenon attributable to the combined action of multiple factors and we are currently pursuing the identification and characterization of each of them.

6. Conclusions and future perspectives

To conclude, in my thesis I was able to:

- demonstrate the specificity of LNA-204 for miR-204, its intended target, and not for miR-211, although the two miRNAs belong to the same family;
- validate the antiproliferative and proapoptotic effects of LNA-204 *in vitro* and in *in vivo* model systems, proving that they are specifically due to the inhibition of miR-204, and not of miR-211;
- demonstrate that LNA-204, through the inhibition of miR-204, induces apoptosis of melanoma cells in a dose-dependent manner (*in vitro*);
- measure the activity of caspases 3/7, 8 and 9 and show that the apoptotic phenotype is triggered by both (intrinsic and extrinsic) pathways;
- demonstrate that a positive correlation exists between the apoptosis induced by LNA-204 and the induction of p53 signaling (stabilization).

Based on the data obtained and discussed, the work will continue with the analysis of the genes identified by RNA-seq (ATP2A1, IQCN, RCVRN, ACTA1, MYH3) in order to find a direct target of miR-204 (by means luciferase assay) or alternatively define the role of each, following miRNA inhibition. If I manage to identify at least one target, I will have to validate its role, as a mediator of apoptosis, both *in vitro* and *in vivo*, inhibiting or overexpressing its expression. In addition, I will have to experimentally demonstrate why the gene of interest is a target of miR-204, but not of miR-211. For this purpose, using specific bioinformatic tools, the MREs (microRNA response elements) present in the entire sequence (5' UTR, CDS and 3' UTR) of each single gene will be analysed. Once specific MREs for miR-204 are identified, mutations will be introduced and the luciferase assay will be repeated to understand if and which site is responsible for the target-miR-204 interaction.

In the meantime, I will continue to study the possible mechanisms through which apoptosis is triggered. As regards the SERCA1(ATP2A1)-p53 binding, I will have to investigate the colocalization between the two proteins in the endoplasmic reticulum by extracting the reticulum membrane and detecting the increased presence of p53 upon LNA-204 transfection by western blot. Eventually, I will confirm the results by immunofluorescence.

I will characterize the genes related to adhesion/migration. I will perform the migration experiment to understand the effect of miRNA inhibition on this process and I will analyse the expression of molecules that mediate cell-cell or cell- matrix adhesion.

Furthermore, I will comprehend whereas TRPM3 plays a role in the examined phenomenon proving the increment in protein levels after miR-204 inhibition as reported in [22]. If the results are encouraging, I will treat melanoma cells with an activator (Pregnenolone sulphate) and a chemical inhibitor (Mefenamic acid) of the calcium channel and I will evaluate the proapoptotic effect, also in combination with LNA-204.

Finally, I will repeat the Time Lapse in order to consolidate the involvement of calcium signaling, particularly, the increment in calcium level after the transfection of LNA-204 and, if the results are confirmed, I will try to understand if and how calcium affects the explored mechanisms in order to provide an answer to the scientific question: "*how does LNA-204 trigger apoptotic cell death?*"

References

1. Leonardi GC, Falzone L, Salemi R, Zanghì A, Spandidos DA, Mccubrey JA, et al. Cutaneous melanoma: From pathogenesis to therapy (Review). Int J Oncol. Spandidos Publications; 2018. p. 1071–80.
2. Dzwierzynski WW. Melanoma Risk Factors and Prevention. Clin Plast Surg. W.B. Saunders; 2021. p. 543–50.
3. Anaba EL. Comparative study of cutaneous melanoma and its associated issues between people of African decent and Caucasians. Dermatol Ther. Blackwell Publishing Inc.; 2021.
4. RASTRELLI M, TROPEA S, ROSSI CR, ALAIBAC M. Melanoma: Epidemiology, Risk Factors, Pathogenesis, Diagnosis and Classification. In Vivo (Brooklyn) [Internet]. 2014;28:1005. Available from: http://iv.iiarjournals.org/content/28/6/1005.abstract
5. Lin JY, Fisher DE. Melanocyte biology and skin pigmentation. Nature. Nature Publishing Group; 2007. p. 843–50.
6. Fecher LA, Amaravadi RK, Flaherty KT. The MAPK pathway in melanoma. Curr Opin Oncol [Internet]. 2008;20. Available from: https://journals.lww.com/co-oncology/fulltext/2008/03000/the_mapk_pathway_in_melanoma.7.aspx
7. Ascierto PA, Kirkwood JM, Grob J-J, Simeone E, Grimaldi AM, Maio M, et al. The role of BRAF V600 mutation in melanoma [Internet]. 2012. Available from: http://www.translational-medicine.com/content/10/1/85
8. Vlašić I, Horvat A, Tadijan A, Slade N. p53 Family in Resistance to Targeted Therapy of Melanoma. Int J Mol Sci. MDPI; 2023.
9. Flaherty KT, Infante JR, Daud A, Gonzalez R, Kefford RF, Sosman J, et al. Combined BRAF and MEK Inhibition in Melanoma with BRAF V600 Mutations. New England Journal of Medicine. 2012;367:1694–703.
10. Ye Q, Li Z, Li Y, Li Y, Zhang Y, Gui R, et al. Exosome-Derived microRNA: Implications in Melanoma Progression, Diagnosis and Treatment. Cancers (Basel). MDPI; 2023.
11. Bafaloukos D, Gazouli I, Koutserimpas C, Samonis G. Evolution and Progress of mRNA Vaccines in the Treatment of Melanoma: Future Prospects. Vaccines (Basel). 2023;11.
12. Xu Z, Fisher DE. mRNA melanoma vaccine revolution spurred by the COVID-19 pandemic. Front Immunol. Frontiers Media S.A.; 2023.
13. Cuciniello R, Filosa S, Crispi S. Novel approaches in cancer treatment: preclinical and clinical development of small non-coding RNA therapeutics. Journal of Experimental and Clinical Cancer Research. BioMed Central Ltd; 2021.
14. Hill M, Tran N. miRNA interplay: Mechanisms and consequences in cancer. DMM Disease Models and Mechanisms. Company of Biologists Ltd; 2021.
15. Mumford SL, Towler BP, Pashler AL, Gilleard O, Martin Y, Newbury SF. Circulating microRNA biomarkers in melanoma: Tools and challenges in personalised medicine. Biomolecules. MDPI AG; 2018.

16. Díaz-Martínez M, Benito-Jardon L, Alonso L, Koetz-Ploch L, Hernando E, Teixido J. miR-204-5p and miR-211-5p contribute to BRAF inhibitor resistance in melanoma. Cancer Res. 2018;78:1017–30.
17. Vignard V, Labbe M, Marec N, Andre-Gregoire G, Jouand N, Fonteneau JF, et al. MicroRNAs in tumor exosomes drive immune escape in melanoma. Cancer Immunol Res. 2020;8:255–67.
18. Dong L, Tian X, Zhao Y, Tu H, Wong A, Yang Y. The Roles of MiRNAs (MicroRNAs) in Melanoma Immunotherapy. Int J Mol Sci. MDPI; 2022.
19. Fattore L, Costantini S, Malpicci D, Ruggiero CF, Ascierto PA, Croce CM, et al. MicroRNAs in melanoma development and resistance to target therapy [Internet]. 2017. Available from: www.impactjournals.com/oncotarget
20. Vitiello M, Tuccoli A, D'aurizio R, Sarti S, Giannecchini L, Lubrano S, et al. Context-dependent miR-204 and miR-211 affect the biological properties of amelanotic and melanotic melanoma cells [Internet]. 2017. Available from: www.impactjournals.com/oncotarget
21. Li T, Pan H, Li R. The dual regulatory role of miR-204 in cancer. Tumor Biology. Springer Science and Business Media B.V.; 2016. p. 11667–77.
22. Hall DP, Cost NG, Hegde S, Kellner E, Mikhaylova O, Stratton Y, et al. TRPM3 and miR-204 Establish a Regulatory Circuit that Controls Oncogenic Autophagy in Clear Cell Renal Cell Carcinoma. Cancer Cell. 2014;26:738–53.
23. Yang F, Bian Z, Xu P, Sun S, Huang Z. MicroRNA-204-5p: A pivotal tumor suppressor. Cancer Med. John Wiley and Sons Inc; 2023. p. 3185–200.
24. Luan W, Qian Y, Ni X, Bu X, Xia Y, Wang J, et al. miR-204-5p acts as a tumor suppressor by targeting matrix metalloproteinases-9 and B-cell lymphoma-2 in malignant melanoma. Onco Targets Ther. 2017;10:1237–46.
25. Shi Y, Liu Z, Lin Q, Luo Q, Cen Y, Li J, et al. Mirnas and cancer: Key link in diagnosis and therapy. Genes (Basel). MDPI; 2021.
26. Braasch DA, Corey DR. Locked nucleic acid (LNA): ¢ne-tuning the recognition of DNA and RNA [Internet]. Available from: http://www.isip.com
27. Grünweller A, Grünweller G, Hartmann RK. Locked Nucleic Acid Oligonucleotides The Next Generation of Antisense Agents? Biodrugs. 2007.
28. Hagedorn PH, Persson R, Funder ED, Albæk N, Diemer SL, Hansen DJ, et al. Locked nucleic acid: modality, diversity, and drug discovery. Drug Discov Today. Elsevier Ltd; 2018. p. 101–14.
29. Nicoli S, Presta M. The zebrafish/tumor xenograft angiogenesis assay. Nat Protoc. 2007;2:2918–23.
30. Vitiello M, Evangelista M, Di Lascio N, Kusmic C, Massa A, Orso F, et al. Antitumoral effects of attenuated Listeria monocytogenes in a genetically engineered mouse model of melanoma. Oncogene. 2019;38:3756–62.
31. Chen TW, Wardill TJ, Sun Y, Pulver SR, Renninger SL, Baohan A, et al. Ultrasensitive fluorescent proteins for imaging neuronal activity. Nature. 2013;499:295–300.
32. Hong BS, Ryu HS, Kim N, Kim J, Lee E, Moon H, et al. Tumor suppressor miRNA-204-5p regulates growth, metastasis, and immune microenvironment remodeling in breast cancer. Cancer Res. 2019;79:1520–34.

33. Ding M, Lin B, Li T, Liu Y, Li Y, Zhou X, et al. A dual yet opposite growth-regulating function of miR-204 and its target XRN1 in prostate adenocarcinoma cells and neuroendocrine-like prostate cancer cells. Oncotarget. 2015;6.
34. Li W, Jin X, Zhang Q, Zhang G, Deng X, Ma L. Decreased expression of miR-204 is associated with poor prognosis in patients with breast cancer. Int J Clin Exp Pathol [Internet]. 2014;7:3287–92. Available from: https://pubmed.ncbi.nlm.nih.gov/25031750
35. Imam JS, Plyler JR, Bansal H, Prajapati S, Bansal S, Rebeles J, et al. Genomic Loss of Tumor Suppressor miRNA-204 Promotes Cancer Cell Migration and Invasion by Activating AKT/mTOR/Rac1 Signaling and Actin Reorganization. PLoS One. 2012;7.
36. Lee H, Lee S, Bae H, Kang HS, Kim SJ. Genome-wide identification of target genes for miR-204 and miR-211 identifies their proliferation stimulatory role in breast cancer cells. Sci Rep. 2016;6.
37. Findlay VJ, Turner DP, Moussa O, Watson DK. MicroRNA-mediated inhibition of prostate-derived ets factor messenger RNA translation affects prostate-derived ets factor regulatory networks in human breast cancer. Cancer Res. 2008;68:8499–506.
38. Chung TKH, Lau TS, Cheung TH, Yim SF, Lo KWK, Siu NSS, et al. Dysregulation of microRNA-204 mediates migration and invasion of endometrial cancer by regulating FOXC1. Int J Cancer. 2012;130:1036–45.
39. Lam E, Wang X, Shin Y, Zhang S, Morrison H, Sun J, et al. A microRNA contribution to aberrant Ras activation in gastric cancer. Am J Transl Res. 2011;3:209–18.
40. Xia Y, Zhu Y, Ma T, Pan C, Wang J, He Z, et al. MiR-204 functions as a tumor suppressor by regulating SIX1 in NSCLC. FEBS Lett. 2014;588:3703–12.
41. Galasso M, Morrison C, Minotti L, Corrà F, Zerbinati C, Agnoletto C, et al. Loss of miR-204 expression is a key event in melanoma. Mol Cancer. BioMed Central Ltd.; 2018.
42. Palkina N, Komina A, Aksenenko M, Moshev A, Savchenko A, Ruksha T. miR-204-5p and miR-3065-5p exert antitumor effects on melanoma cells. Oncol Lett. 2018;15:8269–80.
43. Wang LH, Wu CF, Rajasekaran N, Shin YK. Loss of tumor suppressor gene function in human cancer: An overview. Cellular Physiology and Biochemistry. S. Karger AG; 2019. p. 2647–93.
44. Brennecke J, Stark A, Russell RB, Cohen SM. Principles of microRNA-target recognition. PLoS Biol. 2005. p. 0404–18.
45. Brancati G, Großhans H. An interplay of miRNA abundance and target site architecture determines miRNA activity and specificity. Nucleic Acids Res. 2018;46:3259–69.
46. Broughton JP, Lovci MT, Huang JL, Yeo GW, Pasquinelli AE. Pairing beyond the Seed Supports MicroRNA Targeting Specificity. Mol Cell. 2016;64:320–33.
47. Gross A, Yin XM, Wang K, Wei MC, Jockel J, Milliman C, et al. Caspase cleaved BID targets mitochondria and is required for cytochrome c release, while BCL-X(L) prevents this release but not tumor necrosis factor-R1/Fas death. Journal of Biological Chemistry. 1999;274:1156–63.
48. Billen LP, Shamas-Din A, Andrews DW. Bid: a Bax-like BH3 protein. Oncogene [Internet]. 2008;27:S93–104. Available from: https://doi.org/10.1038/onc.2009.47

49. Roy S, Nicholson DW. Commentary Cross-Talk in Cell Death Signaling [Internet]. J. Exp. Med. 2000. Available from: http://www.jem.org/cgi/content/full/192/8/F21
50. Hattori Y, Takano KI, Teramae H, Yamamoto S, Yokoo H, Matsuda N. Insights into sepsis therapeutic design based on the apoptotic death pathway. J Pharmacol Sci. Japanese Pharmacological Society; 2010. p. 354–65.
51. Lin YC, Lin JF, Tsai TF, Chou KY, Chen HE, Hwang TIS. Tumor suppressor miRNA-204-5p promotes apoptosis by targeting BCL2 in prostate cancer cells. Asian J Surg. 2017;40:396–406.
52. Ferreira KS, Kreutz C, MacNelly S, Neubert K, Haber A, Bogyo M, et al. Caspase-3 feeds back on caspase-8, Bid and XIAP in type I Fas signaling in primary mouse hepatocytes. Apoptosis. 2012;17:503–15.
53. Ji Z, Njauw CN, Taylor M, Neel V, Flaherty KT, Tsao H. P53 rescue through HDM2 antagonism suppresses melanoma growth and potentiates MEK inhibition. Journal of Investigative Dermatology. 2012;132:356–64.
54. Thiem A, Hesbacher S, Kneitz H, Di Primio T, Heppt M V., Hermanns HM, et al. IFN-gamma-induced PD-L1 expression in melanoma depends on p53 expression. Journal of Experimental and Clinical Cancer Research. 2019;38.
55. Ikediobi ON, Davies H, Bignell G, Edkins S, Stevens C, O'Meara S, et al. Mutation analysis of 24 known cancer genes in the NCI-60 cell line set. Mol Cancer Ther. 2006;5:2606–12.
56. Loureiro JB, Raimundo L, Calheiros J, Carvalho C, Barcherini V, Lima NR, et al. Targeting p53 for melanoma treatment: Counteracting tumour proliferation, dissemination and therapeutic resistance. Cancers (Basel). 2021;13.
57. Marcel V, Fernandes K, Terrier O, Lane DP, Bourdon JC. Modulation of p53β and p53γ expression by regulating the alternative splicing of TP53 gene modifies cellular response. Cell Death Differ. 2014;21:1377–87.
58. Makino E, Gutmann V, Kosnopfel C, Niessner H, Forschner A, Garbe C, et al. Melanoma cells resistant towards MAPK inhibitors exhibit reduced TAp73 expression mediating enhanced sensitivity to platinum-based drugs. Cell Death Dis. 2018;9.
59. Moon SH, Cho MH, Kim MY. Cellular inactivation of nitric oxide induces p53-dependent apoptosis in human melanoma cells. Tropical Journal of Pharmaceutical Research. 2016;15:1595–603.
60. Lavin MF, Gueven N. The complexity of p53 stabilization and activation. Cell Death Differ. 2006. p. 941–50.
61. Nguyen TA, Menendez D, Resnick MA, Anderson CW. Mutant TP53 posttranslational modifications: Challenges and opportunities. Hum Mutat. Wiley-Liss Inc.; 2014. p. 738–55.
62. Zhang L, Hou N, Chen B, Kan C, Han F, Zhang J, et al. Post-Translational Modifications of p53 in Ferroptosis: Novel Pharmacological Targets for Cancer Therapy. Front Pharmacol. Frontiers Media S.A.; 2022.
63. Olsson A, Manzl C, Strasser A, Villunger A. How important are post-translational modifications in p53 for selectivity in target-gene transcription and tumour suppression? Cell Death Differ. 2007. p. 1561–75.
64. Xu H, Van Remmen H. The SarcoEndoplasmic Reticulum Calcium ATPase (SERCA) pump: a potential target for intervention in aging and skeletal muscle pathologies. Skelet Muscle. BioMed Central Ltd; 2021.

65. Dai J, Li Q, Zhou Q, Zhang S, Chen J, Wang Y, et al. IQCN disruption causes fertilization failure and male infertility due to manchette assembly defect . EMBO Mol Med. 2022;14.
66. Flaherty KM, Zozulya S, Stryer L, Mckay DB. Three-Dimensional Structure of Recoverin, a Calcium Sensor in Vision. Cell. 1993.
67. Lacroix M, Toillon RA, Leclercq G. p53 and breast cancer, an update. Endocr Relat Cancer. Society for Endocrinology; 2006. p. 293–325.
68. Sionov RV, Haupt Y. The cellular response to p53: the decision between life and death. Oncogene [Internet]. 1999;18:6145–57. Available from: https://doi.org/10.1038/sj.onc.1203130
69. Giorgi C, Bonora M, Sorrentino G, Missiroli S, Poletti F, Suski JM, et al. P53 at the endoplasmic reticulum regulates apoptosis in a Ca2+-dependent manner. Proc Natl Acad Sci U S A. 2015;112:1779–84.
70. Jang YN, Jung YS, Soo HL, Moon CH, Kim CH, Eun JB. Calpain-mediated N-cadherin proteolytic processing in brain injury. Journal of Neuroscience. 2009;29:5974–84.